ANN model for predicting the direct normal irradiance and the global radiation for a solar application to a residential building

C. Renno*, F. Petito, A. Gatto
Department of Industrial Engineering, University of Salerno,
Via Giovanni Paolo II, 132, 84084 Fisciano (Salerno), Italy.
*Corresponding author: crenno@unisa.it, tel. +39 089964327, fax +39 089964037.

Abstract

An accurate solar potential estimation of a specific location is basic for the solar systems evaluation. Generally, the global solar radiation is determined without considering its different contributes, but systems as those concentrating solar require an accurate direct normal irradiance (DNI) evaluation. Solar radiation variability and measurement stations non-availability for each location require accurate prediction models. In this paper two Artificial Neural Network (ANN) models are developed to predict daily global radiation (GR) and hourly direct normal irradiance (DNI). Two heterogeneous set of parameters as climatic, astronomic and radiometric variables are introduced and the data are obtained by databases and experimental measurements. For each ANN model a multi layer perceptron (MLP) is trained and validated investigating nine topological network configurations. The best ANN configurations for predicting GR and DNI are tested on different new dataset. MAPE, RMSE and R^2 for the GR model are respectively equal to 4.57%, 160.3 Wh/m^2 and 0.9918, while for the DNI they are equal to 5.57%, 17.7 W/m^2 and 0.994. Hence, the proposed models show a good correlation both between measured and predicted data and with the literature. The main results obtained are the DNI and the GR models predicting which have allowed the evaluation of the electric energy production by means of two different photovoltaic systems used for a residential building. Hence, the developed ANN models represent a good tool to support the assessment of the green energy production evaluation.

Key-words: solar energy, artificial neural network, direct normal irradiance and global radiation, photovoltaic systems.

1. Introduction

The solar radiation prediction is a basic aspect in the modeling and performance evaluation of the solar systems (Wild et al., 2015), when the energy demands of different kind of users have to be satisfied (Meade and Islam, 2015). The solar energy can be used in many applications as: electrical energy demand balancing in the national grids, environmental pollution reduction, design and size of integrated energy systems, thermal load analysis in the buildings, atmospheric energy balance studies (Eicker et al., 2015). Sunlight is principally composed by the direct and diffuse components. The solar energy analysis takes usually into account the global solar radiation for a specific location without considering its different contributes. Although the most applications adopt the global radiation, the concentrating photovoltaic systems (CPV) require, generally, an accurate evaluation of the direct normal irradiance (DNI) also for a domestic application (Renno and Petito, 2015). The solar resource data availability can play a strategic role in the solar systems assessment (Qazi et al., 2015). Generally, different measurement equipments are adopted in the solar energy evaluation such as pyranometer, solarimeter and pyroheliometer. The solar radiation variability and the measurement stations non-availability for each location require accurate prediction models which include different variables. This is fundamental when the direct normal irradiance has to be predicted. In particular, the use of an ANN which predicts the DNI could be also a key factor in order to assess the residential CPV/T systems potential (Sharaf and Orhan, 2015). Hence, for the assessment, control and optimization of the solar systems an integrated forecast is necessary, able to consider the different solar radiation components and a temporal level of the prevision from one hour up to one day or one month in advance. So, an accurate evaluation of the solar energy potential for different locations is a basic factor in order to configure a solar system. In particular, it allows to support the evaluation of a cleaner production for different locations, taking into account different components of the solar source. The solar radiation prediction is complex because affected by several variables such as meteorological, climatic and radiometric. Several methods have been developed in order to deal with prediction shortcomings by employing data from different measurements sites (Lazzaroni et al., 2015). Other models can be employed in order to ensure an effective forecasting of the solar energy amount for different locations.

There are empirical (Loutzenhier et al., 2007), numerical and statistical models (Noorian et al., 2008) or physical models. In literature there are different examples of physical models which principally employ several linear equations for the solar radiation prediction. These works exploit decomposition models (Yao et al., 2015), atmospheric parameters (Polo et al., 2016) or meteorological analysis (Kambezidis et al.,2016). Anyway they do not always guarantee an accurate prediction when the solar energy varies hour by hour or day by day.

A very interesting solution adopts an artificial intelligence which represents a good tool in order to solve non-linear problems. The Artificial Neural Network (ANN) models allow to investigate tasks which depend on many physical phenomena and are also employed for a large variety of applications such as: classification, data mining, pattern recognition, image compression, process modeling, etc (Linares-Rodriguez et al., 2013). ANNs adopt long-term data series, working as a "black box" and obtaining a higher level of reliability in order to carry out a non-linear mapping. ANN techniques are alternative methods to traditional models in order to predict the solar energy potential for different locations (Sahin et al., 2013; Hasni et al., 2012). In particular, the ANN models can estimate the solar radiation and its components. Hence, the global solar radiation or the direct one can be exploited as function of the solar system characteristics. The ANN use in renewable energy systems has initially been reviewed by Kalogirou (Kalogirou, 2001), and then, it has been applied for several energy system analyzes. As for the thermal analysis and heat exchanger (Mohanraj et al., 2015), for energy analysis of buildings (Kumar et al., 2013) and for solar radiation prediction (Yadav and Chandel, 2014). Many studies concerning the solar energy prediction by means of ANNs have been developed involving several parameters as function of the target application and the data availability; the main literature results are presented in Section 2, focusing on the ANN configuration in terms of selected input and topologic characterization. In this paper two ANN models have been investigated in order to forecast the daily global solar radiation (GR) and the hourly DNI for University of Salerno (Fisciano, 40°46’23’’N, 14°47’52’’E). Different set of heterogeneous parameters such as climatic, astronomical and radiometric variables have been introduced for the ANNs. The data have been obtained adopting databases and experimental measurements, then they have been trained and tested by a multi layer perceptron (MLP) analyzing several kinds of network topological configurations. In particular, each ANN model has been realized investigating nine different network configurations. The best topological configuration of the ANN for predicting daily GR and DNI has been validated with different sets of new data, including different locations; the results have been compared with different ANN models present in the literature. The ANN model results have been employed in order to compare two different photovoltaic systems adopted for a residential building. Hence, the models have been applied to a residential case study, analyzing their impact in terms of a cleaner energy production of different renewable systems. The paper is organized as follow; in Section 2 different literature examples for the prediction of solar radiation by means of ANN are described. Section 3 shows the methodology used in order to develop the ANNs, while the ANN configurations for daily GR and hourly DNI are presented in Section 4. In Section 5 the results for the investigated models are reported showing the selected configurations for each ANN. Moreover, exploiting the ANN predictions, a comparison between two photovoltaic systems for a residential application is presented. Finally, the conclusions are given in Section 6.

2. ANN literature review for modeling the solar energy potential

ANNs represent a mathematical tool used for a wide tasks variety. The ANN modeling allows to carry out the required output starting from corresponding input vectors without considering the assumption of any determinate relationship between the input and output (Celik and Muneer, 2012). ANNs operate principally adopting the interconnection of a neurons number which represent localized processing centers between input and output layers. Hence, they work as "black box" employing distinct features such as: input, hidden and output layers of neurons, training functions for the learning process from a set of past data, transfer functions between layers that allow the information flow. There are many types of connection for the data transfer, the most used is the multi layer perceptron (MLP) (Chen et al., 2013). It is a feed-forward ANN where data flow from input layer to the output layer without any feedback.

In literature many ANNs have been developed for the GR predicting, while the DNI estimation has been less investigated (Teke et al., 2015). A significant number of studies about the GR modeling and forecasting by means of ANNs has been undertaken, offering a wide range of possibilities which differ for number and type of input variables considered (Yadav et al., 2014), time level of the analysis and network configuration. In Table 1 a literature analysis on ANN for predicting solar radiation is reported together with the main characteristics of the neural networks developed; in particular, for each analyzed paper, a list of advantages and disadvantages has been reported. Many models for the solar radiation estimation are developed taking into account a monthly input (Qazi et al., 2015). Azadeh et al. have developed a multilayer feed-forward network in order to estimate monthly the GR for six cities in Iran adopting climatic and meteorological data collected for six years

(Azadeh et al., 2009). Wang et al. estimate the hourly GR exploiting data of the National Renewable Energy Laboratory (NREL), collected in four years (Wang et al., 2011). The transfer functions are respectively, for the hidden and the output layer, hyperbolic tangent and sigmoid. Khatib et al. employ a MLP that estimates the clearness index in order to calculate the daily GR and the diffuse solar irradiation for different stations (Khatib et al., 2012). Data of twenty-eight stations have been collected: twenty-three stations for the network training and five for its testing. The global solar radiation estimation by means of ANN models requires the analysis of the input parameters. Yadav et al. have employed the Rapid Miner technique for input variable selection in order to predict the solar radiation using different ANN techniques, such as radial basis function (RBF) and generalized regression ANN (Yadav et al., 2015). Celik et al. evaluate the ANN potential in order to estimate the global solar radiation from different variation of input parameters in Eastern Mediterranean Region of Turkey (Celik et al., 2016). Behrang et al. have developed a MLP and a radial basis function based on six combinations of the inputs reported (Beharang et al., 2010). The data have been taken between 2002 and 2006 for Dezful city in Iran (32°16'N, 48°25'E). The measured data between 2002 and 2005 are used to train the neural networks, while the data from 2006 represent the test set. A RBF is also investigated by Zervas el al. trying to use the minimum number of inputs such as the weather conditions and the duration of daylight (Zervas et al., 2008). Gairaa et al. have investigated a combined approach to the solar radiation prediction coupling Box-Jenkings and ANN models (Gairaa et al., 2016). Benghanem and Mellit have investigated a MLP and a RBF for predicting the daily GR (Benghanem and Mellit, 2010). They have used four different input combinations. Data have been collected by NREL from 1998 to 2002 at Al-Madinah (Saudi Arabia). Yacef et al. have developed a classical ANN and different Bayesian Neural Networks (BNN) for estimating the daily GR (Yacef et al., 2012). Amrouche and Privert developed two models that exploit the local forecasting data; hence, the two ANNs can predict the GR for locations where the measurements are not possible (Amrouche and Privert, 2014). Moreover, Bilgili and Ozgoren have modeled the daily GR in Adana, city of Turkey, by means of a multi-linear regression (MLR), a multi-nonlinear regression (MNLR) and a MLP artificial neural network (Bilgili and Ozgoren, 2011). Finally, the solar potential estimation of western Himalayan Indian state of Himachal Pradesh is conducted by Yadav and Chadel, employing the J48 algorithm for the selection of input parameters for ANN model. They have established that the most relevant input parameters are temperature, altitude and sunshine hours and developed five ANN models for the GR estimation (Yadav and Chandel, 2015).

The ANN can also be used for the DNI prediction in order to assess the solar systems that operate only with the solar radiation direct component (Renno and De Giacomo, 2014) as the concentrating photovoltaic systems (Renno, 2014). Yadav and Chandel have reviewed different ANN techniques for the solar radiation evaluation, but techniques able to estimate the DNI have been not considered (Yadav and Chadel, 2014). A MLP neural network has been investigated, by Mellit et al., to evaluate the hourly DNI and to compare it with an adaptive model (Mellit et al., 2013). A feed-forward ANN has also been applied by Kuashika et al. for the clearness index evaluation of the DNI, collecting data by eleven stations in India (Kaushika et al., 2014). Finally, clearness index has also been evaluated with ANN model by Kheradmand et al. by considering environmental and meteorological factors (Kheradmand et al., 2016). So, different ANN models for the global radiation prediction have been developed in literature. They use principally a specific set of input parameters and don’t investigate the different topology solutions. On the other hand, ANN models have been not implemented specifically for the hourly DNI.

In this paper, on the contrary, two neural networks are presented; they allow the GR and DNI prediction by means of a set of heterogeneous parameters. In particular, astronomical variables, generally not considered, combined to other types of variables, radiometric and climatic, have been adopted to estimate GR and DNI. Moreover, the DNI is not considered in many papers that are focused on GR and its different estimation tools (MLP, RBF, regression models, adaptive models, BNN etc.). In addition, in this paper the part of choice of the best network is deepened showing the process that allows to realize different alternatives of the network and the choice. Finally, respect to many papers present in literature the network results are used for a practical application.. In particular the estimated data for daily GR and hourly DNI are respectively employed for the energy comparison between the PV and CPV systems.

3. ANN models development method

The ANN modeling for mapping non-linear problems requires the implementation of different steps. Each phase is characterized by the choice of features which impact both on previous and subsequent steps (Khatiba et al., 2012). A statistical analysis has been conducted in order to select the right ANN topological configuration for predicting daily GR and hourly DNI. The ANN designing involves the definition of inputs, type of network, topology, training paradigm and transfer functions. In particular, the modeling process can be basically divided in three steps. The first considers the topology network design taking into account the input parameters, the ANN type, the number of hidden layers and neurons. This step also involves the choice of the training algorithm, the transfer functions and the training and validation samples. The second step constitutes the training phase where the samples are implemented in the ANN models in order to adjust weights and biases as function of a predetermined condition. The last step is the validation, the ANN models are tested with a new set of data and their accuracy can be evaluated by means of statistical parameters.

The developed methodology is based on two main aspects. The first is related to the use of a heterogeneous set of unconventional input variables such as meteorological, radiometric, astronomical and geographical parameters for the daily GR and hourly DNI prediction. The second considers the network architecture; hence, each model has been performed after training and validating of nine different topological configurations. Hence, the input selection constitutes the first aspects examined, since it allows the successive network topological analysis. A statistical analysis, based on the times-series, has been conducted for the selection of the type and the number of input variables. The time series is a collection of observations ordered in the time, each one recorded at a specific time. In the first approximation, a time series model assumes that the past patterns will occur in the future. In fact, a time series model could be used only to provide a synthetic time series similar statistically to the original one. The modeling of the series begins with the selection of a suitable mathematical model for the data. The artificial neural networks are intelligent systems that have the capacity to learn, memorize and create relationships among data. They could represent a non-linear tool for time series modeling (Voyant et al., 2013). In order to determine which of the exogenous and endogenous parameters have to be considered in the ANN models a correlation measure is computed for the input variables. The correlation between two variables reflects the degree by which the variables are linked. The most common correlation measure is the Pearson’s correlation. A correlation of +1 (or -1) means that there is a perfect positive (or negative) linear relationship between variables and a value of 0 implies that there is no linear correlation between the variables. The Pearson correlation coefficient (R) between two variables is defined by covariance and variance of the two variables. For a series the estimation of R is given by:

$$R = \frac{\sum_{K=1}^{n}(x_k-\bar{x})\,(y_k-\bar{y})}{\sqrt{\sum_{K=1}^{n}(x_k-\bar{x})^2\,\sum_{K=1}^{n}(y_k-\bar{y})^2}} \qquad (1)$$

The significance of each variables x has been correlated to the output of interest y: the daily GR for the first ANN model and the hourly DNI for the second ANN model.

Hence, after choosing the model exogenous and endogenous variables, considering the time-series analysis, an optimization process, which has evaluated the best network configuration for the daily GR and the hourly DNI, has been conducted. Generally, the features involved in the recombination process are the type of transfer functions, the number of hidden layers and the number of hidden neurons. All these configurations expect a feed-forward network such as the MLP one. The training, validation and test data have been obtained by experimental measurements and database for different locations. The models accuracy is evaluated by means of the validation results for the nine topological network configurations. The statistical indicators employed for comparison are mean squared error (MSE), root mean squared error (RMSE), mean absolute percentage error (MAPE), mean absolute error (MAE) and goodness of fit (R^2).

They are given by the following relationships:

$$\mathrm{MSE} = \frac{1}{n}\sum_{i=1}^{n}(y_i - \hat{y}_i)^2 \qquad (2)$$

$$\mathrm{RMSE} = \sqrt{\frac{1}{n}\sum_{i=1}^{n}(y_i - \hat{y}_i)^2} \qquad (3)$$

$$\mathrm{MAPE} = \frac{1}{n}\sum_{i=1}^{n}\frac{|\hat{y}_i - y_i|}{y_i} \qquad (4)$$

$$\mathrm{MAE} = \frac{1}{n}\sum_{i=1}^{n}|y_i - \hat{y}_i| \qquad (5)$$

$$R^2 = \frac{\sum_{i=1}^{n}(\hat{y}_i - \bar{y})^2}{\sum_{i=1}^{n}(y_i - \bar{y})^2} \qquad (6)$$

where n is the cardinality of dataset involved in the analysis, y_i is the variable to estimate, $\bar{y}$ is the mean value of y_i and $\hat{y}_i$ is the value calculated by the model. MAPE determines the accuracy and RMSE represents the standard deviation between predicted values and actual values; it is a good parameter to compare the forecasting error of different models related to the same variable. MAE measures as the predictions are close to observed values, while R^2

calculates the ratio between the variation evaluated by a regression model and the sample data variation; R^2 is an important parameter since it evaluates the general accuracy of a regression model. The best configurations both for daily GR and hourly DNI are tested with different set of data and the results are compared with models present in literature. In Figure 1 the main steps of the proposed method for the ANN model development are reported. The same procedure is applied to estimate daily GR and hourly DNI in order to define, finally, the solar energy potential for a solar system located at University of Salerno.

4. ANN models for daily GR and hourly DNI

In this section the elements of the ANNs used for the solar energy potential modeling are described. The main aim is to develop an accurate model for predicting GR and DNI, in order to evaluate the solar potential for solar systems application located at University of Salerno (Fisciano, 40°46’23’’N, 14°47’52’’E). In this paper, the neural network tool of MATLAB (Matlab, LTD) has been used for the models implementation. For both models the selected architecture is constituted by a feed-forward neural network trained with Levenberg – Marquardt (LM) algorithm. The MLP learning rule adopted is the error Back-Propagation (BP) algorithm. It calculates the gradient of the network error related to its modifiable weights. The BP learning approach can be implemented considering different topologies and transfer functions. This typical problem, during the ANN development, is solved by means of the cross-validation which is a validation technique to estimate how a model generalizes an independent data set. First of all, the input variables have been selected exploiting the correlation factor (R) and the time series; then, also the number of input variables has been evaluated by means of a statistical comparison based on normalized RMSE. Once defined the input sets, nine different configurations are investigated for both ANNs in order to choose the configuration that assures the best performances. The network architecture, the paradigm and the learning algorithm of the ANNs has been fixed thanks to the information of the literature that has clearly indicated MLP, BP and LM, as reported in Table 1. The values of the transfer function, the number of hidden neurons and the number of hidden layers have been changed considering a set of plausible values. The different pairs of transfer functions, for the hidden layer and the output layer, have been chosen referring to the literature where for the output layer the linear function is often chosen. So, the transfer function of the hidden layer should necessarily be non-linear and the sigmoid function is chosen because allows better results respect to tanh as reported in some simulations, conducted in Matlab, where the networks compared were the same except for the hidden layer transfer function. The functions tanh-tanh have been chosen because, after some tests where it only the MSE has been determined, the function tanh, both for the hidden layer and for the output layer, presents the best results considering two non-linear function instead of one.

Finally, assuming to use one hidden layer or two hidden layers, thanks to the results of the approximation theorem universal, several combinations of the transfer functions have been investigated, using two hidden layers, and by means of simulations in Matlab. These simulations have shown only the MSE trend and its final value, and, at the end, has been chosen tanh-tanh-linear as a combination of transfer functions that give the best results, referring respectively to the first hidden layer, the second and the output layer. On the contrary, as regards the number of hidden neurons, for the network which estimates the GR, a low number of neurons has been initially considered, 8, until the simulations have given decreasing values of MSE, using only one hidden layer. In fact, the simulations has been interrupted when 12 hidden neurons have given worst performance than 10. But for defining this number of neurons, the performance of the networks and of those for which the increase of the neurons number seemed to give improvements, or at least results comparable, has been deepened. The same has been made with the two hidden layers and for the network which estimates the DNI. At the end, combining different values, nine different configurations have been obtained for both networks. The data have been obtained between 2013, 2014 and 2015 by means of experimental measurements and database, taking into account different locations. The data are divided in three subsets, the first represents the training set used to compute the gradient and to update the network weights and biases by means of the training algorithm. The second is the validation set which calculates the error avoiding overfitting; the early stopping technique is used in order to improve the network generalization capability. This technique saves network weights and biases when the minimum validation error is reached. The validations results allow to select the best configurations, which are tested by means of the third data set (test set) in order to confirm the networks predictive power. The data treatment represents a key point in order to build the ANN models, because a big amount of data of different locations and years has been employed. They have been obtained from databases and exploiting a set of experimental measurements. All the employed data have been pre-processed in order to have a training phase that would lead to a correct generalization as fast as possible. In particular, abnormal values or outlier have been excluded. This set of data represents values which completely differ from all other obtained values. Hence, they have been not considered in order to avoid a wrong influence during the training phase. As suggested by (Muneer , 2004), the outliers have been excluded calculating the first and third percentile, and evaluating the following data range:

$$[\mathrm{Q}_1 - \mathrm{k}(\mathrm{Q}_3 - \mathrm{Q}_1), \mathrm{Q}_3 + \mathrm{k}(\mathrm{Q}_3 - \mathrm{Q}_1)] \qquad (7)$$

where Q_i represents the percentile and k is a constant value, set to 1.5. The data not included in the range obtained by means of the Equation 7, have been excluded because they have been considered outliers (Muneer, 2004). Then, the data have been normalized in the range [-1,1]. The normalization represents a good tool when a big set of data without outliers is available. In fact, the presence of outliers could lead to misalignments in the training phase because most of the data will be concentrated in a small range. The use of the normalization rather than the standardization allows to avoid the variables measurement units and the range magnitude influence in the training phase. Moreover, exploiting the sigmoid function during the training phase, it has been necessary a small range of values because this function already reaches its asymptote with an input equal to 3 or -3. Hence, when the net input is greater than three at the beginning of the training process, the gradients will be very small, and the network training will be very slow. (Azadeh et al. 2008; Wang et al. 2011). Abnormal values appear for two reasons due to the kind of data obtained. The first reason depends on the database data which can be affected by the measurement errors. The second reason depends on the measurement station in Salerno; in fact, for a certain period there have been some measurement problems from which this abnormal values derive. By means of the Matlab function “mapminmax”, the normalization interval [-1,1] is defined. At the end of the test phase, the “mapminmax” function is also used in post-processing with the purpose to put outputs into original domain.

4.1. ANN implementation for predicting the daily GR

The daily GR prediction has been performed adopting database values of different locations and measurements for the target site of University of Salerno. In particular, the database considered includes a mix of climatic and meteorological values obtained by the Agro-meteorological Regional Center (Campania Region, 2014) referring to four specific locations: Sessa Aurunca (41°14’N, 13°56’E), Greci (41°15’10’’N, 15°10’12’’E), Montemarano (40°54’58’’N, 14°59’54’’E) and Policastro Bussentino (40°04’06’’N, 15°31’05’’E). The experimental measurements, especially employed for the validation and test set construction, have been obtained by means of a pyranometer, with a measuring and spectral range respectively equal to 0-2000 W/m^2 and 335-2200 nm, and a platinum thermo-resistance. The target location and its surroundings stations for data collection are shown in Figure 2.

The input set selection constitutes a key factor in the model implementation. The correlation analysis for the input variables in order to predict the daily GR has been reported in Table 2. In particular, a set of nine heterogeneous parameters have been considered: latitude (Lt), longitude (Lg), mean temperature (T), sunshine duration (SD), total precipitation (P), daylight hours (H) declination angle (δ). wind speed (WS) and humidity (Hu). As reported in Table 2, the most effectiveness input parameter is sunshine duration, which is a radiometric parameter and gives an indication about the location cloudiness (Yadav and Chadel, 2012). SD is defined as the sum of sub-period when the solar irradiance exceeds 120 W/m^2 (Benghanem and Joraid, 2007). In order to define a model for the GR in different locations, geographic variables such as latitude and longitude have been included also if their correlation is low. Wind speed, humidity and precipitation usually allow to characterize the meteorological situation (Wang et al., 2011). Anyway, wind speed and humidity have been found to be the least incident and they have been not considered. Finally, there are two astronomical variables such as the daylight hours and declination angle. The first defines the period of the year considered, considering also the important information about the cloudiness especially if it is compared with the sunshine duration. The second takes into account the specific day considered. They have been evaluated by means of analytic expressions (Renno and Petito, 2013). Once defined the input variables, considering the correlation value, their number has been chosen. Different ANNs have been trained and validated by changing the number of input variables and evaluating their nRMSE (normalized root mean squared error) value. In Table 3 all the analyzed combinations for the daily GR have been reported together with the respective value of nRMSE. It can be noted that the network with seven input variables (latitude (Lt), longitude (Lg), mean temperature

(T), sunshine duration (SD), total precipitation (P), daylight hours (H) and declination angle (δ)) reaches the best results for the daily GR model. Hence, the daily GR can be written in this way:

$$\mathrm{GR} = \mathrm{f}(\mathrm{Lt}, \mathrm{Lg}, \mathrm{T}, \mathrm{SD}, \mathrm{P}, \mathrm{H}, \delta) \quad (8)$$

Once defined the input set, different topological network configurations are trained and validated varying different features. In particular, for this model a training set of ten months has been chosen while the validation set considers three months. Nine configurations are investigated from GR1 to GR9 as shown in Table 4. The number of hidden layers, hidden neurons and the transfer functions type are charged in order to obtain an accurate predicting model. The solutions proposed expects principally one or two hidden layers; the transfer functions analyzed are sigmoid, linear and hyperbolic tangent. They describes how the information flow both from the input to the hidden layer and from the hidden layer to the output. The best configuration, resulting from the statistical analysis, is tested on different test sets. A first set considers as testing location the University of Salerno, collecting data for March, July and November 2014. In order to prove the good prediction capability of the GR model, other test sets are employed. In particular, respect to the first test set, different locations and years are considered: the four stations (Sessa Aurunca, Policastro Bussentino, Montemarano, Greci) used for training, with data from 2013 to 2014, are selected also in the test phase. Data for January, March and June 2015 are introduced for testing the proposed ANN. The proposed neural network calculates the outputs as follow:

$$\mathrm{y_k} = \mathrm{f}\left\{\left[\sum_{\mathrm{j}=1}^{\mathrm{Z}} \mathrm{w_j} \mathrm{g}\left(\left(\sum_{\mathrm{i}=1}^{7} \mathrm{p_{ji}} \mathrm{x_{ik}}\right) + \mathrm{b_j}\right)\right] + \mathrm{a}\right\} \ \text{ with } |\mathrm{K}| = \mathrm{No.\,patterns} \quad (9)$$

where f and g are respectively the output layer and the hidden layer transfer functions adopted, p_{ji} is the weights matrix of hidden neurons j and input neurons i, w_j is the vector of weights referred to the hidden neurons j and the output neuron, z is the number of hidden neurons, x_{ik} is the matrix of input, b_i is the vector of hidden neurons biases, a is the value of the output neurons bias, y_k is the value of the output for k-th day.

4.2. ANN implementation for forecasting the hourly DNI

The DNI forecasting represents an important aspect for a full solar energy potential evaluation. While global radiation measurements are usually obtained in most of the radiometric stations, the data availability of its components is more limited. Moreover, when the DNI is measured, there is no extensive data series. Mathematical models are need in order to establish a typical behavior of the direct solar resources for energy applications. The DNI analysis for a specific location is often calculated starting from the global irradiance data registered. It is estimated by means of the decomposition model based on the regression between two indices: the clearness index k_t (horizontal global irradiance/horizontal extraterrestrial irradiance) and the direct solar transmittance k_b (direct normal irradiance/extraterrestrial irradiance) (Lopez et al., 2005). Anyway, the DNI evaluation is affected by the increasing complexity due to relationship non-linearity between the variables on which it depends (Gueymard et al., 2011). Hence, traditional statistical methods are not efficient. The ANN can exploit a mix of experimental data and calculated values for the DNI prediction. An ANN model to evaluate the hourly DNI is introduced investigating different solutions.

To overcome the lack of experimental data, a measurement system has been installed at University of Salerno. The data have been obtained with a sampling interval of one hour. The measurements refer to the direct irradiance by means of a pyrheliometer; other necessary data are related to the global irradiance on a normal plane and air temperature, part of this data have been also exploited for the global radiation predicting. The training data are referred to six months, while the validation subset is of two months. As for the GR model, the DNI model analysis starts with the input set definition. In Table 5, the correlation analysis of four astronomical and radiometric variables: clearness index (k_t), declination angle (δ), hour angle (HRA) and global normal irradiance (G_{ni}) is reported, and it can be observed as the global normal irradiance (G_{ni}) reaches a values very close to 1.

In Table 6, different combinations of these variables have been indicated together with the respective value of nRMSE and the better solution is represented by the use of all the indicated variables:

$$\mathrm{DNI} = \mathrm{f}\,(\mathrm{k_t}, \delta, \mathrm{HRA}, \mathrm{G_{ni}}) \tag{10}$$

The declination angle and hour angle allow the ANN training considering information about the day considered and its sunlight duration. In particular, the HRA influences the optical path length through the atmosphere; hence, it can replace the relative air mass. The clearness index represents the most relevant factor in the DNI prediction. The clearness index is defined as the ratio between the horizontal global irradiance and the horizontal extraterrestrial irradiance. It constitutes an indirect measure of the atmosphere filtering action. Last variables included is the global normal irradiance which provides information about the meteorological and climatic effects in the evaluation process. As in the previous case, the LM algorithm has been adopted for the network training, due to its better performance (Sfetsos and Coonick, 2000). Nine topologic network configurations (DNT1-DNT9) are simulated on validation subset as shown in Table 7. The best configuration is finally tested on a test subset of one month. The output of the proposed neural network for the prediction of the hourly DNI is calculated as:

$$\mathrm{y_k} = \mathrm{f}\left\{\left[\sum_{j=1}^{z} \mathrm{w_j} \mathrm{g}\left(\left(\sum_{i=1}^{4} \mathrm{p_{ji}} \mathrm{x_{ik}}\right) + \mathrm{b_j}\right)\right] + \mathrm{a}\right\} \text{ with } |\mathrm{k}| = \mathrm{No.\,patterns} \tag{11}$$

5. Results and discussion

The proposed methodology provides three different levels of analysis. After the input selection and the preliminary network configuration, for each ANN model nine topological schemes are trained and validated. The first step allows the best configuration definition as function of RMSE, MAPE, MAE and R^2. In the second phase the selected configurations are tested and their results are evaluated. The third step expects the comparison between the developed stable models and literature. The models constitute an integrated tool for the solar energy potential estimation at University of Salerno. Moreover, the ANN model for daily GR has been implemented taking into account different locations; hence, it allows the GR estimation for each site. The model of the hourly DNI has been obtained by investigating a great amount of data and parameters. Anyway, the lack of experimental data for the hourly direct solar irradiance for other locations different from Salerno, has not allowed a test phase for other location. So, even if it is limited to the selected location, the DNI prediction by ANN results more accurate than classical methods based on different equations that do not take into account some factors such as the cloudiness. Hence, the predicted values are closer to the measured values than the calculated one allowing a detailed analysis because it is hourly. The test of the DNI ANN has been conducted taking into account a hourly temporal level characterized by weather variations; hence it represents a more reliable test that has shown the accuracy of the model.

5.1 Selected configurations for ANN models and testing results

The solar energy potential estimation is affected by the networks forecasting capabilities for daily GR and hourly DNI. The evaluation of the solar energy main components allows different solar energy system assessment. Hence, it is possible to determine the effectiveness potential for systems based on the exploitation of the global and direct radiation. The uniqueness of the present ANN modeling approach is that it investigates the network predicting power analyzing nine topological configurations for each ANN model.

Hence, the neural models are initially constructed based on preliminary choices such as the input set selection and the training algorithm definition, and after the recombination process, illustrated in Figure 2, they are performed in order to obtain a more accurate prediction. The main aspects analyzed in the recombination process have concerned the transfer function type, the number of hidden layers and hidden neurons.

The ANN model for daily the GR estimation has been determined implementing three types of transfer functions for the hidden layer and the output layer: sigmoid, linear and hyperbolic tangent. Two solutions in term of hidden layers have been investigated: one or two layers. The hidden neurons number has been varied between a minimum of eight and a maximum of twelve. In Table 8, the statistical results for the nine topological configurations have been reported. The selected ANN network is GNT2 which expects one hidden layer, ten hidden neurons, a sigmoid transfer function for the hidden layer and a linear for the output layer. This configuration presents the best results in term of RMSE, MAPE and MAE, respectively equal to 153.5 Wh/m^2, 4.46% and 125.7 Wh/m^2. Although the R^2 values are not the best in absolute terms, GNT2 has showed a better overall predicting power, as reported in the scatterplots of Figure 3. The scatterplots show important indications referring to the correlation between measured and predicted data. Hence, the good agreements achieved between previsions and measured values are clearly proved for GNT2 (Figure 3b), other scatterplots refer respectively to GNT1 (a), GNT6 (c) and GNT7 (d). Hence, a solution with two hidden layers (GNT7) or 12 hidden neurons (GNT6) shows both RMSE and MAPE higher than the selected one with only one hidden layer and ten hidden neurons.

As for the hourly DNI, the topological solutions have been investigated considering one or two hidden layers, sigmoid, linear and hyperbolic tangent transfer functions and a number of hidden neurons between four and six. In Table 9 the validation results for hourly DNI configurations are reported. DNT5 has been found as the best solution for all statistical parameters adopted. Its RMSE, MAPE, MAE and R^2 values are respectively equal to 17.1 W/m^2, 5.38%, 13.4 W/m^2 and 0.9956. The same result can be observed in Figure 4, where the predicted and measured data have been compared for DNT3 (a), DNT5 (b), DNT6 (c) and DNT8 (d). In Figures 3 and 4 only four graphs are shown instead of nine since only some aspects have been displayed. These aspects are three: the effect of the neurons number increase, the use of two non-linear transfer functions instead of one, and finally use of two hidden layers. These effects have been outlined, respectively, for the GR, in the transition between GNT1 and GNT2 and then considering GNT6 (use-tanh tanh) and GNT7 (uses two hidden layers). The same has been done for the DNI. Hence, it has been chosen only the number of graphs necessary to show these aspects avoiding to display the other part that has a similar trend. The proposed ANNs structures for daily GR and hourly DNI are reported in the Figures 5a and 5b (Gairaa et al., 2016; Yadav et al., 2015; Alsina et al. 2016; Shaddel et al. 2016). The ANN for DNI presents four input neurons and a hidden layer with five neurons.

The good results obtained by the selected topological configurations for GR model and DNI model, can be observed also in the Figures 6a and 6b. In particular, these scatterplots show the regression respect to the target in the training phase. The trend between predicted and measured values, during the training for the selected configuration (GNT2) of the daily GR network and for the selected configuration (DNT 5) of the hourly DNI model reflect the good achievements of the subsequent validation phase.

The selected ANN model configurations for GR and DNI have been tested on the respective test subset previously defined. The test step for daily GR has been developed referring to different locations and years. In particular, a first test set refers to March, July and November

2014 for the target location of University of Salerno. These months have been selected because they present different climatic conditions. In Figure 7 the comparison between predicted and measures values for the GR have been reported. So, for the different months considered the ANN model estimates with high correlation the global radiation. Based on test set results, MSE, MAPE, MAE, R^2, RMSE and nRMSE have been used as statistical indicators. These parameters present values higher than the validation results. This result is partially expected because the validation and test data are different; moreover, in order to evaluate the network prediction capability, the test set has been chosen with months characterized by a greater heterogeneity. Anyway, results show good correlation with a MAPE of 4.57%, a RMSE of 160.3 Wh/m^2 and a R^2 of 0.9918. In order to support the good prediction capability of the developed ANN model for daily GR, new test sets, considering different locations, have been employed. In particular, new data for January, March and June 2015 have been considered for the four locations (Sessa Aurunca, Montemarano Policastro, Greci, Bussentino) employed in the training phase with data from 2013 to 2014. In Figure 8, the trend between predicted and measured values for the new locations and months are reported as scatterplot figures. Once again, the results show high correlation as confirmed by the calculated statistical results. In particular, the RMSE, MAPE and R^2 are respectively of 212 Wh/m^2, 8.1% and 0.9831 for Sessa Aurunca (a); 135 Wh/m^2, 5.21% and 0.9911 for Montemarano (b); 122 Wh/m^2, 4.1% and 0.9926 for Greci (c) and 173 Wh/m^2, 5.71% and 0.9884 for Policastro Bussentino (d).

As for the DNI test step, the trend of the predicted and measured values, referred to April 2014, has been illustrated in Figure 9. The forecast capabilities of the ANN model for the hourly DNI has been confirmed by means of the calculated MAPE, RMSE and R^2, which are respectively equal to 5.57%, 17.7 W/m^2 and 0.994. These values guarantee correlation and good accuracy to forecast the DNI when astronomical and radiometric variables are adopted. The main aim of this paper concerns the DNI predicting with neural network. The model allows the direct solar energy potential assessment for the selected location; hence, it could be useful for the evaluation of a concentrating solar system. The model forecasting capability for the hourly DNI estimation can be observed in Figure10. The ANN has been simulated with reference to a summer and winter day with different meteorological situations. In particular, it can be observed the model availability to predict the DNI, taking into account the cloudiness as reported by the input set variables. Finally, in Table 10 cumulating data on monthly base, the fraction of direct radiation has been estimated. Table 10 reports the cumulated on a monthly base values of global and direct radiation obtained by means of the neural network models. Anyway, considering a low value of the albedo component, the diffuse radiation can also be estimated. Hence, already considering a monthly basis of analysis, the diffuse radiation has also been indicated in Table 10. It can be observed in terms of monthly radiation that the percentage of direct radiation increases to 90% in summer period, while it decreases to 80% in winter.

5.2 Application of the ANN models to a residential building

The solar radiation prediction, both in term of global radiation and direct normal irradiance, allows the energy production evaluation of different solar systems. In particular, it can represent a good tool for the assessment of a system for a cleaner energy production. The ANNs designed in this paper for a specific Italian location ensure an accurate solar potential prediction in order to compare different solar solutions for a residential building. In particular, while many accurate estimations of the solar global radiation are available thanks to different solar calculators and measurement stations, the data availability of the DNI for a specific place is more limited. Hence, the ANN model realized in this paper represents a good tool to estimate the actual solar potential of a specific location and to guarantee a good assessment for different solar systems. So, a case study represented by the feasibility analysis of a trigenerative CPV/T system adopted in the Southern Italy, is shown. This case study, even if it is theoretical, represents an important aspect to open new scenarios, also considering experimental aspect, related to the use of the solar energy.

The selected case study is related to a residential building of about 130 m^2. The analysis is based on the comparison between a traditional photovoltaic system (PV) and an innovative concentrating photovoltaic and thermal system (CPV/T), principally in term of electric energy production. Both systems have been designed in order to meet the electric energy demand of the residential application. In particular, the CPV/T system allows also to meet part of the thermal and cooling energy demands of the building. The energy loads of the residential building considered are reported in Table 11.

The traditional PV system has been sized taking into account a total peak power of 3 kW, typical for a domestic user; hence, twelve silicon modules of 0.250 kW have been used. The CPV/T system represents an evolution in the photovoltaic field. The main characteristic is to concentrate sunlight in order to increase the incident direct solar radiation and to decrease the photovoltaic area. For this purpose, it adopts optical devices able to modify the concentration factor defined as:

$$C = \frac{A_{opt}}{A_c} \cdot \eta_{opt} \tag{12}$$

where A_{opt} and A_c represent respectively the optics and cell area, and η_{opt} the optical efficiency which depends on the optic device adopted. These systems adopt triple junction cells able to operate at high temperature, and a tracking system since they can work only with the direct component of the solar radiation.

The designed CPV/T system considers a point-focus configuration where each optics, represented by a small parabolic dish, presents a InGaP/InGaAs/Ge triple-junction solar cell placed in its focus. The cells are arranged on a pipe where a cooling fluid, usually a water–glycol solution, flows in order to cool the cells and to obtain simultaneously thermal energy.

According to the total electric energy demand, the CPV/T system has been sized considering 150 Emcore triple junction cells (Emcore, 2012) of 1 cm^2 arranged in three modules of fifty. The comparison between the two different photovoltaic systems has been carried out adopting the monthly results of the ANN model for the global and direct radiation, as reported in Table 10.

The monthly electric energy of a traditional PV system can be expressed by:

$$E_{el,PV,m} = [(GR_m \cdot \eta_{PV})] \cdot n_{mod} \cdot \eta_{inv} \tag{13}$$

where GR_m is the monthly global radiation presented in Table 6, η_{PV} represents a standard efficiency value for a silicon photovoltaic module equal to 13% (Mastrullo and Renno, 2010), n_{mod} is the number of modules used and the inverter efficiency (η_{inv}) is generally considered equal to 0.90 (Aprea and Renno, 2009).

The CPV/T system monthly electric energy production can be estimated as:

$$E_{el,CPV/T,m} = E_{c,m} \cdot n_c \cdot \eta_{mod} \cdot \eta_{inv} \tag{14}$$

where the module efficiency (η_{mod}) until 100 cells is equal to 0.9, n_c represents the number of cells which constitute the module and η_{inv} is the inverter efficiency. The monthly electric energy of the cell $E_{el,c,m}$ can be expressed as:

$$E_{el,c,m} = DNI_m \cdot C \cdot A_c \cdot \eta_{opt} \cdot \eta_c \tag{15}$$

where DNI_m represents the monthly direct radiation reported in Table 10; C is the concentration factor while η_{opt} and η_c are respectively the optic and cell efficiency.

The CPV/T system presents a concentration factor of 800; the optic efficiency, taking into account small parabolic dishes, has been considered equal to 0.865 (Brogen, 2004), while the cell efficiency is fixed to 31% according to the cell manufacturer instructions (Emcore, 2012) and the references values for this type of cell (Green et al., 2014).

In Figure 11, the electric energy demand and the monthly electric energy production both for PV and CPV/T system are reported. The annual electric energy production of the PV system is equal to 3030 kWh, while the production of the CPV/T system is equal to 2996 kWh. Hence, both systems allow to meet the electric energy yearly demands of the residential building. On the other hand, a CPV/T system allows to obtain also thermal energy that can be expressed by:

$$E_{th,CPVT} = \{[1 - (\eta_c \cdot \eta_m \cdot \eta_{opt})] \cdot C \cdot DNI \cdot A_c \cdot n_c\} - E_{th,loss} \tag{16}$$

where the annual thermal energy production considered takes into account an annual value of DNI and a thermal energy loss due to convective and radiative losses included between 3-5% (Kribus et al., 2006). In Table 11 both the monthly electric and thermal energy production of the CPV/T system and the PV system electric production are reported together with the residential building energy demand. The CPV/T system allows an annual thermal energy production of 10655 kWh_{th} that can be employed both for the sanitary hot water (SHW) production and the cooling demands. In particular, an absorber heat pump (AHP) with a peak power of about 7 kW_{coo} has been considered for the summer cooling (Aprea and Renno, 1999). Hence, both photovoltaic systems allow a cleaner energy production ensuring an important contribution in reducing environmental pollution. The different systems have been also evaluated from an economic point of view, considering the systems capital costs and the electric and thermal energy savings. The PV system presents a average cost of 5.4 k€ (Balcombe et al. 2015), with a simple pay-back (SPB) of about 8 years. The CPV/T system shows an initial cost of 6.2 k€, with a SPB of about 9 years considering only the electric energy savings and the cash flows opportunely evaluated (Renno and Petito, 2015). The CPV/T system thermal production meets the SHW needs and the cooling demands employing the AHP. Considering an AHP cost of about 350 €/kW_{coo} (Eicker and Pietruschka, 2009), the CPV/T system total cost is equal to 8650 €. Analyzing the thermal and cooling energy savings in this new configuration and the respective cash flows, the SPB of the CPV/T system decreases to about 7 years. Hence, the CPV/T system results competitive with the PV system and it can represent a trigenerative solution for a residential building application.

5.3 Literature comparison

In the last years several techniques have been developed for predicting the solar energy potential. The presented ANN models have been compared with different models present in literature in terms of statistical indicators. This analysis allows an external validation of the developed ANNs for predicting daily GR and hourly DNI. In particular, the compared values for the daily GR model takes into account the statistical results for the test set of Salerno. The statistical parameter values obtained in correspondence of each GR and DNI prediction model are summarized in Table 12. Azadeh et al. estimated the monthly GR for six cities in Iran using climatic and meteorological data collected for six years (Azadeh et al., 2009). The model presents different values both for each statistical indicator and each city. The best performances are shown with reference to the city of Bandar Abbas with MAPE, R^2 and nRMSE respectively equal to 3.00%, 0.980 and 2.60%. The two ANN models for hourly GR, developed by Wang et al., present R^2 and nRMSE values respectively equal to 0.991 and 3.31% for the first configuration and 0.964 and 4.50% for the second (Wang et al., 2011).

In the models investigated by Khatib et al., the best MAPE and nRMSE values for the predicted GR, between the different networks developed are 5.2% and 7.96%, while the best RMSE is 342.0 Wh/m^2 (Khatib et al., 2012). The MLP model developed by Behrang et al. has shown MAPE and R^2 equal respectively to 5.21% and 0.9957, while their RBF for the same chosen input configuration has reported a MAPE of 5.56% and a R^2 of 0.9952 (Behrang et al., 2010). The RBF model by Zervas et al. is only compared in term of R^2, reaching a value of 0.985 (Zervas et al. 2008). The best results by Benghanem and Mellit, have been obtained using a RBF model with the day of the year, the sunshine duration and the air temperature as input parameters (Benghanem and Mellit, 2010). In this case, R^2 is 0.976 and nRMSE is 1.31%. The Bayesian Neural Network (BNN) developed by Yacef et al. in order to estimate the daily GR shows better results than a classic ANN with R^2 and nRMSE respectively equal to 0.9299 and 8.42% (Yacef et al., 2012). Bilgili and Ozgoren have modeled the daily GR with different models. The ANN method has presented better statistical results: MAE is 278 Wh/m^2, MAPE is 9.23% while R^2 is 0.9508 (Bilgili and Ozgoren, 2011). Hence, the comparison between the proposed ANN model for daily GR and literature model has clearly proved the good accuracy of the developed tool and has validated the results with good agreement.

In literature, the GR estimation in the energy applications is widely investigated by means of ANNs, while the DNI prediction is not present with the same diffusion. Hence, the ANN for predicting hourly DNI is only compared with the models presented by Mellit et al. (Mellit et al., 2013) and Kaushika et al. (Kaushika et al., 2014). In Table 12, the statistical indicators calculated for the hourly DNI modeling are also reported. The analysis has been developed comparing the R^2 value with Mellit et al. model and the RMSE achieved with the Kaushika et al. network. The first has presented a R^2 of 0.967, lower than the proposed model value. The second according to the R^2 value has showed a feed-forward neural network less accurate than the proposed one. Hence, both the ANNs presented in this paper have shown high performances comparable with the outputs presented in literature.

6. Conclusions

In this paper a tool based on ANNs has been developed in order to estimate the solar energy potential of the University of Salerno. Two ANN models have been investigated to predict the daily GR and the hourly DNI. The proposed ANN development has been subdivided in different steps. First, the methodology has adopted a feed-forward network with a set of heterogeneous variables and LM algorithm as training function. Data have been collected for over two years considering both experimental data and databases. Successively, for both solar components, nine topological network configurations have been validated. The validation results have been compared in term of RMSE, MAPE, MAE and R^2. The selected ANN for the daily GR expects one hidden layer, ten hidden neurons, a sigmoid transfer function for the hidden layer and a linear function for the output layer. A neural network with sigmoid and linear transfer functions, one hidden layer and five hidden neurons, has been chosen for the hourly DNI forecasting. The MLP realized for the GR has been able to predict the radiation for different locations using radiometric, climatic, meteorological and astronomical parameters, while the model of the DNI has principally employed radiometric and astronomical values only for the target site. The GR model considers four locations for training and it is tested referring to different locations and years. As for the DNI model the test phase can be realized only for the place where the experimental data have been collected. The ANN model for the hourly direct irradiance, couldn't be tested on other locations due to the lack of experimental or database data for the direct irradiance. However, the methodology for the development of two networks for the GR and DNI prediction is valid and can represent the basis for subsequent models.

Finally, the best configurations selected for each model have been tested on new data and the results have been compared with the literature. The predictive ability comparison obtained by means of statistical indicators, however, represents a tool independent of the conditions and that then has allowed to compare different situations. The evaluation of different statistical indicators has showed that the ANN models presented can estimate daily GR and hourly DNI with satisfactory accuracy. In particular, the ANN for the GR has presented a MAPE of 4.57%, a RMSE of 160.3 Wh/m^2 and a R^2 of 0.9918, which have guaranteed a good correlation between predicted and measured values. The ANN forecasting capabilities related to the hourly DNI have been confirmed obtaining the MAPE, RMSE and R^2 values respectively equal to 5.57%, 17.7 W/m^2 and 0.994. The network for predicting the direct irradiance represents an important result, because in literature there are few papers that determine the DNI. In particular, the use of the heterogeneous inputs set adopted in this paper has never been presented in literature.

The direct irradiance has been evaluated for various climatic conditions characterized by different levels of cloudiness. Moreover, the direct fraction has been predicted on monthly base reaching obviously the higher values in the summer period. Finally, the DNI predicting model has allowed to evaluate for a residential building the energy production of two different photovoltaic systems. In particular, the CPV/T system is resulted competitive with the PV system and it can represent an interesting trigenerative solution for a residential application. Therefore, the developed ANN models could represent a good tool for the assessment of cleaner energy system, ensuring a correct evaluation of the solar source potential for different location.

Nomenclature

a	output layer bias
A	area
AHP	absorber heat pump
ANN	Artificial Neural Network
AV	average
b_j	vector of hidden layer biases
BP	back propagation
c	cell
C	concentration factor
CPV/T	concentrating photovoltaic and thermal
DNI	Direct Normal Irradiance (W/m^2)
E	electric energy (kWh)

f	output layer transfer function
GR	global radiation (Wh/m^2)
g	hidden layer transfer function
H	daylight hours (h)
Hu	humidity
HRA	hour angle (°)
k	constant
k_b	direct solar transmittance
k_t	clearness index
L_g	longitude (°)
LM	Levenberg-Marquardt
L_t	latitude (°)
MAE	mean absolute error
MAPE	mean absolute percentage error
MLP	multilayer perceptron
MLR	multi linear regression
MNLR	multi non linear regression
MSE	mean squared error
NREL	national renewable energy laboratory
p_{ij}	array of hidden layer weights
P	precipitation (mm)
PV	photovoltaic
Q	percentile
R^2	goodness of fit
RMSE	root mean squared error

RH	relative humidity
RTD	resistance temperature detector
SD	sunshine duration (h)
SHW	sanitary hot water
T	temperature (°C)
VP	vapor pressure
w_j	vector of output layer weights
WS	wind speed
x	variable of interest
x_i	input array
n	cardinality of dataset
y	variable to estimate
$\overline{y}$	mean value of the variable to estimate
$\hat{y}$	estimated value of the variable to estimate
z	number of hidden neurons

Greek symbol

δ	solar declination angle (°)
η	efficiency

Subscripts

CPV/T	concentrating photovoltaic and thermal
coo	cooling
el	electric
inv	inverter
m	monthly
mod	module

ni normal irradiance

opt optic

PV photovoltaic

th thermal

References

Alsina, E.F., Bortolini, M., Gamberi, M., Regattieri, A., 2016. Artificial neural network optimisation for monthly average daily global solar radiation prediction. Energy Conversion and Management 120, 320–329.

Amrouche, B., Le Privert, X., 2014. Artificial neural network based daily local forecasting for global solar radiation. Applied Energy 130, 333-341.

Aprea C., Renno, C., 1999. An air cooled tube-fin evaporator model for an expansion valve control law. Mathematical and Computer Modelling 30, 135-146.

Aprea, C., Renno, C., 2009. Experimental model of a variable capacity compressor. International Journal of Energy Research 33, 29-37.

Azadeh, A., Ghaderi, S.F., Sohrabkhani, S., 2008. A simulated-based neural network algorithm for forecasting electrical energy consumption in Iran. Energy Policy 36, 2637–2644

Azadeh, A., Maghsoudi, A., Sohrabkhani, S., 2009. An integrated artificial neural networks approach for predicting global radiation. Energy Conversion and Management 50, 1497–1505.

Balcombe, P., Rigby, D., Azapagic, A., 2015. Energy self-sufficiency, grid demand variability and consumer costs: Integrating solar PV, Stirling engine CHP and battery storage. Applied Energy 155, 393:408.

Behrang, M.A., Assareh, E., Ghanbarzadeh, A., Noghrehabadi, A.R., 2010. The potential of different artificial neural network (ANN) technique in daily global solar radiation modeling based on meteorological data. Solar Energy 84, 1468–1480.

Benghanem, M., Joraid, A.A., 2007. A multiple correlation between different solar parameters in Medina, Saudi Arabia. Renewable Energy 14, 2424–2435.

Benghanem, M., Mellit, A., 2010. Radial Basis Function Network-based prediction of global solar radiation data: Application for sizing of a stand-alone photovoltaic system at Al-Madinah, Saudi Arabia. Energy 35, 3751-3762.

Bilgili, M., Ozgoren, M., 2011. Daily total global solar radiation modeling from several meteorological data. Meteorol. Atmos. Phys. 112, 125–138.

Brogen. M., 2004. Optical Efficiency of Low-Concentrating Solar Energy Systems with Parabolic Reflectors. Acta Universitatis Upsaliensis. Uppsala, Sweden, Ph.D. Thesis.

Campania Region Study; Available online; http://www.sito.regione.campania.it /agricoltura/meteo/agrometeo, (Accessed on 16 December 2014).

Celik, A.N., Muneer, T., 2012. Neural network based method for conversion of solar radiation data. Energy Conversion and Management 51, 117-124.

Celik, O., Teke, A., Basak Yldirim, H., 2016. The optimized artificial neural network model with LevenbergeMarquardt algorithm for global solar radiation estimation in Eastern Mediterranean Region of Turkey. Journal of Cleaner Production 116, 1-12.

Chen, S.X., Gooi, H.B., Wang, M.Q., 2013. Solar radiation forecast based on fuzzy logic and neural networks. Renewable Energy 60, 195-201.

Eicker, U., Demir, E., Gürlich, D., 2015. Strategies for cost efficient refurbishment and solar energy integration in European Case Study buildings. Energy and Buildings 102, 237–249.

Eicker, U., Pietruschka, D., 2009. Design and performance of solar powered absorption cooling systems in office buildings. Energy Build. 41, 81–91.

Green, M., Emery, K., Hishikawa, Y., Warta, W., Dunlop, E.D., 2014. Solar cell efficiency tables. Prog. Photovolt: Res. Appl. 22, 701–710.

Gueymard, C.A., Stephen, M., Wilcox, S.M., 2011. Assessment of spatial and temporal variability in the US solar resource from radiometric measurements and predictions from models using ground-based or satellite data. Solar Energy 85, 1068-1084.

Gairaa, K., Khellaf, A., Messlem, Y., Chellali, F., 2016. Estimation of the daily global solar radiation based on Box–Jenkins and ANN models: A combined approach. Renewable and Sustainable Energy Reviews 57, 238-249.

Hasni, A., Sehli, A., Draoui, B., Bassou, A., Amieur, B., 2012. Estimating global solar radiation using artificial neural network and climate data in the south-western region of Algeria. Energy Procedia 18, 531 – 537.

Kalogirou, S.A., 2001. Artificial neural networks in renewable energy systems applications: a review. Renewable and Sustainable Energy Reviews 5, 373–401.

Kambezidis, H.D., Psiloglou, B.E., Karagiannis, D., Dumka, U.C., Kaskaoutis, D.G., 2016. Recent improvements of the Meteorological Radiation Model for solar irradiance estimates under all-sky conditions. Renewable Energy 93, 142-158.

Kaushika, N.D., Tomar, R.K., Kaushik, S.C., 2014. Artificial neural network model based on interrelationship of direct, diffuse and global solar radiations. Solar Energy 103, 327–342.

Khatib, T., Mohamed, A., Sopian, K., Mahmoud, M., 2012. Solar Energy Prediction for Malaysia Using Artificial Neural Networks. International Journal of Photoenergy 12, 16 pages.

Khatiba, T., Mohameda, A., Sopian, K., 2012. A review of solar energy modeling techniques. Renewable and Sustainable Energy Reviews 16, 2864– 2869.

Kheradmand, S., Nematollahi, O., Reza Ayoobi, A., 2016. Clearness indexpredictingusinganintegratedartificial neuralnetwork (ANN) approach. Renewable and Sustainable Energy Reviews 58, 1357-1365.

Kribus, A., Kaftori, D., Mittelman, G., Hirshfeld, A., Flitsanov, Y., Dayan, A., 2006. A miniature concentrating photovoltaic and thermal system. Energy Conversion and Management 47, 3582-3590.

Kumar, R., Aggarwal, R.K., Sharmaa, J.D., 2013. Energy analysis of a building using artificial neural network: A review. Energy and Buildings 65, 352–358.

Lazzaroni, M., Ferrari, S., Piuri, V., Salman, A., Cristaldi, L., Faifer, M., 2015. Models for solar radiation prediction based on different measurement sites. Measurement 63, 346–363.

Linares-Rodriguez, A., Ruiz-Arias, J.A., Pozo-Vazquez, D., Tovar-Pescador, J., 2013. An artificial neural network ensemble model for estimating global solar radiation from Meteosat satellite images. Energy 61, 636-645.

Lopez, G., Batlles, F.J., Tovar-Pescador, J., 2005. Selection of input parameters to model direct solar irradiance by using artificial neural networks. Energy 30, 1675–1684.

Loutzenhier, P.G., Manz, H., Felsmann, C., Strachan, P.A., Frank, T., Maxwell, G.M., 2007. Empirical validation of models to compute solar irradiance on inclined surfaces for building energy simulation. Solar Energy 81, 254–67.

Mastrullo, R., Renno, C., 2010. A thermoeconomic model of a photovoltaic heat pump. Applied Thermal Engineering 30, 1959-1966.

MATLAB R2007b, 1994–2015 The Math Works, Inc., Massachusetts (United States).

Meade, N., Islam, T., 2015. Modelling European usage of renewable energy technologies for electricity generation. Technological Forecasting & Social Change 90, 497–509.

Mellit, A., Eleuch, H., Benghanem, M., Elaoun, C., Massi Pavan, A., 2013. An adaptive model for predicting of global, direct and diffuse hourly solar irradiance. Energy Conversion and Management 67, 117–124.

Mohanraj, M., Jayaraj, S., Muraleedharan, C., 2015. Applications of artificial neural networks for thermal analysis of heat exchangers - A review. International Journal of Thermal Sciences 90, 150-172.

Muneer, T., 2004. Solar Radiation and Daylight Models. Second Edition, Elsevier.

Noorian, A.M., Moradi, I., Kamali, G.A., 2008. Evaluation of 12 models to estimate hourly diffuse irradiation on inclined surfaces. Renewable Energy 33, 1406–12.

Polo, J., Ballestrín, J., Carra, E., 2016. Sensitivity study for modelling atmospheric attenuation of solar radiation with radiative transfer models and the impact in solar tower plant production. Solar Energy 134, 219–227.

Qazi, A., Fayaz, H., Wadi, A., Raj, R.G., Rahim, N.A., Khan, W.A., 2015. The artificial neural network for solar radiation prediction and designing solar systems: a systematic literature review. Journal of Cleaner Production 104, 1-12.

Renno, C., 2014. Optimization of a concentrating photovoltaic thermal (CPV/T) system used for a domestic application. Applied Thermal Engineering 67, 396-408.

Renno, C., De Giacomo, M., 2014. Dynamic simulation of a CPV/T system using the finite element method. Energies 7, 7395-7414.

Renno, C., Petito, F., 2013. Design and modeling of a concentrating photovoltaic thermal (CPV/T) system for a domestic application. Energy and Buildings 62, 392–402.

Renno, C., Petito, F., 2015. Choice model for a modular configuration of a point-focus CPV/T system. Energy and Buildings 92, 55-66.

Sahin, M., Kaya, Y., Uyar, M., 2013. Comparison of ANN and MLR models for estimating solar radiation in Turkey using NOAA/AVHRR data. Advances in Space Research 51, 891–904.

Sfetsos, A., Coonick, A.H., 2000 Univariate and multivariate forecasting of hourly solar radiation with artificial intelligence techniques. Solar Energy 68, 169–178.

Shaddel, M., Javan, D.S., Baghernia, P. 2016. Estimation of hourly global solar irradiation on tilted absorbers from horizontal one using Artificial Neural Network for case study of Mashhad. Renewable and Sustainable Energy Reviews 53, 59–67.

Sharaf, O.Z., Orhan, M.F., 2015. Concentrated photovoltaic thermal (CPVT) solar collector systems: Part II - Implemented systems, performance assessment, and future directions. Renewable and Sustainable Energy Reviews, 50, 1566-1633.

Teke, A., Yıldırım, H.B., Çelik, Ö., 2012. Evaluation and performance comparison of different models for the estimation of solar radiation. Renewable and Sustainable Energy Reviews 50, 1097–1107.

Triple-Junction Solar Cell for Terrestrial Applications, CTJ Photovoltaic Cell – 10 mm x 10 mm, Datasheets Emcore September 2012, Emcore Corporation.

Voyant, C., Muselli, M., Paoli, C., Nivet, M.L., 2013. Hybrid methodology for hourly global radiation forecasting in Mediterranean area. Renewable Energy 53, 1-11.

Wang, Z., Wang, F., Su, S., 2011. Solar Irradiance Short-Term Prediction Model Based on BP Neural Network. Energy Procedia 12, 488-494.

Wild, M., Folini, D., Henschel, F., Fischer, N., Muller, B., 2015. Projections of long-term changes in solar radiation based on CMIP5 climate models and their influence on energy yields of photovoltaic systems. Solar Energy 116, 12–24.

Yacef, R., Benghanem, M., Mellit, A., 2012. Prediction of daily global solar irradiation data using Bayesian neural network: A comparative study. Renewable Energy 48, 146-154.

Yadav, A.K., Chandel, S.S., 2012. Artificial neural network based prediction of solar radiation for Indian stations. Int. Journal of Computer Applications 50, 1-4.

Yadav, A.K., Chandel, S.S., 2014. Solar radiation prediction using Artificial Neural Network techniques: A review. Renewable and Sustainable Energy Reviews 33, 772–781.

Yadav, A.K., Chandel, S.S., 2015. Solar energy potential assessment of western Himalayan Indian state of Himachal Pradesh using J48 algorithm of WEKA in ANN based prediction model. Renewable Energy 75, 675-693.

Yadav, A.K., Malik, H., Chandel, S.S., 2014. Selection of most relevant input parameters using WEKA for artificial neural network based solar radiation prediction models. Renewable and Sustainable Energy Reviews 31, 509–519.

Yadav, A.K., Malik, H., Chandel, S.S., 2015. Application of rapid miner in ANN based prediction of solar radiation for assessment of solar energy resource potential of 76 sites in Northwestern India. Renewable and Sustainable Energy Reviews 52, 1093-1106.

Yao, W., Li, Z., Xiu, T., Lu, Y., Li, X., 2015. New decomposition models to estimate hourly global solar radiation from the daily value. Solar Energy 120, 87-99.

Zervas, P.L., Sarimveis, H., Palyvos, J.A., Markatos, N.C.G., 2008. Prediction of daily global solar irradiance on horizontal surfaces based on neural-network techniques. Renewable Energy 33, 1796–1803.

Figure captions

Figure 1 Proposed methodology for ANN models development

Figure 2 Target location and its measurement stations for data collection

Figure 3 Scatterplots of four different ANN configurations for predicting the daily GR

Figure 4 Scatterplots of four different ANN configurations for predicting the daily DNI

Figure 5 Structure of the proposed neural networks for daily global radiation (a) and hourly direct irradiance (b)

Figure 6 Regression respect to the target in the training phase: (a) GR model GNT2, (b) DNI model DNT5

Figure 7 Comparison between measured and predicted daily GR values for University of Salerno

Figure 8 Comparison between measured and predicted daily GR values for different locations: (a) Sessa Aurunca, (b) Montemarano, (c) Greci, (d) Policastro Bussentino

Figure 9 Comparison between measured and predicted hourly DNI values

Figure 10 Hourly DNI in different climatic conditions

Figure 11 Electric energy demand of the residential building and monthly electric energy production of the PV and CPV/T systems

Table captions

Table 1 ANN characteristics summary of the literature analysis

Table 2 Correlation analysis for GR model input

Table 3 Number of input and nRMSE for the GR model

Table 4 Different topology configurations of the ANN model for daily GR

Table 5 Correlation analysis for DNI model input

Table 6 Number of input and nRMSE for the DNI model

Table 7 Different topology configurations of the ANN model for hourly DNI

Figure

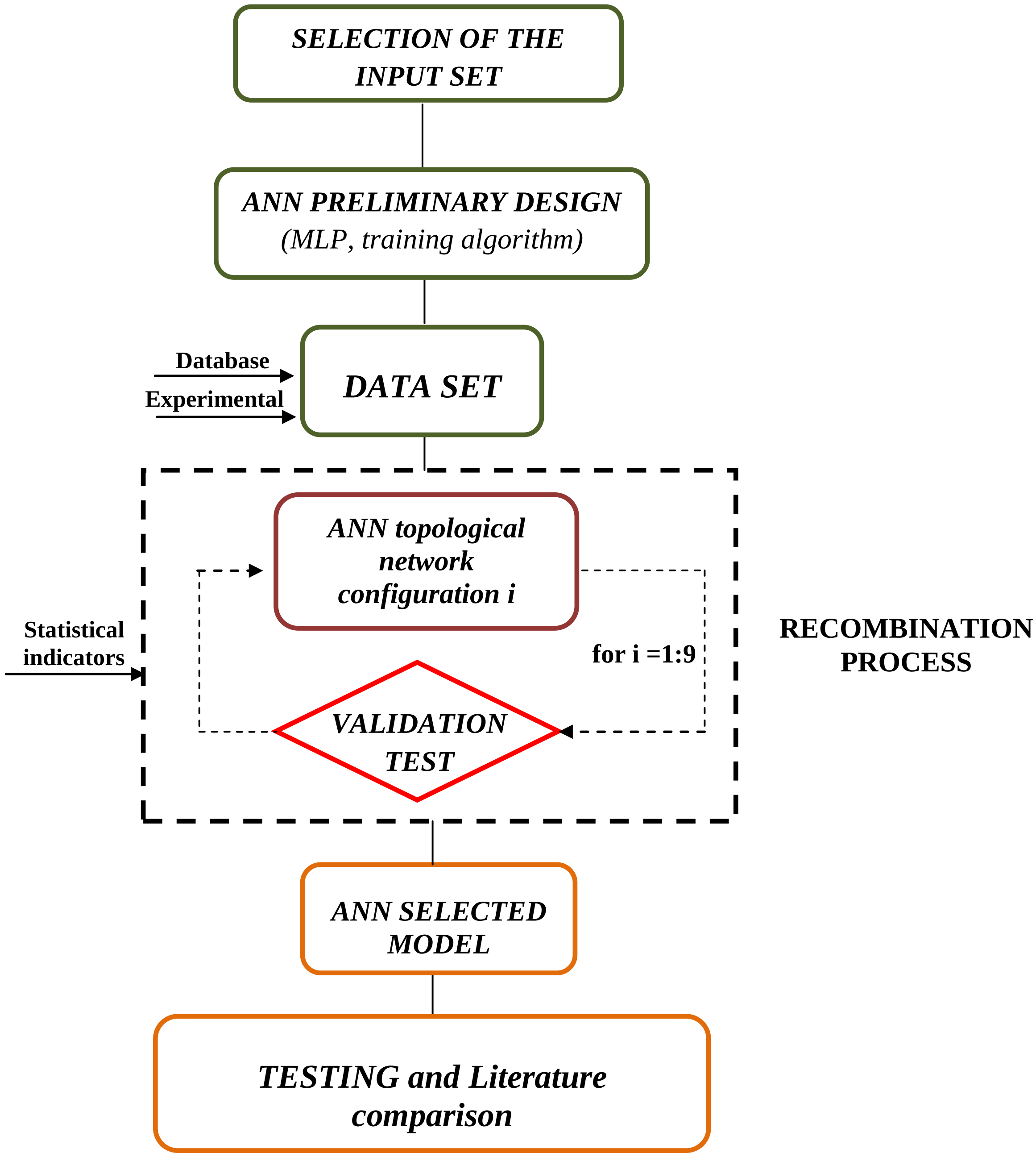

Figure 1 Proposed methodology for ANN models development

Figure

Figure 2 Target location and its surrounding measurement stations for data collection

Figure

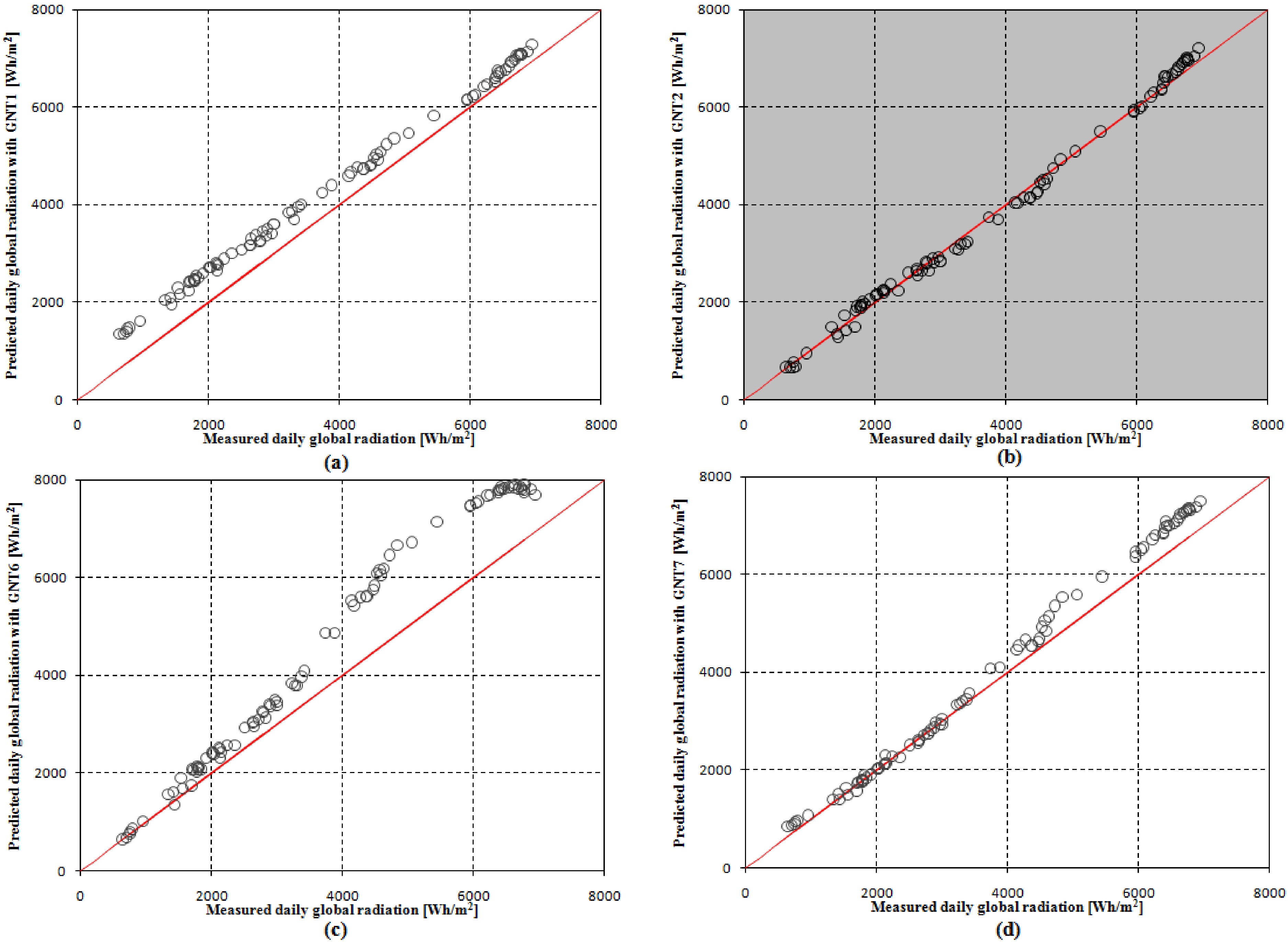

Figure 3 Scatterplots of four different configurations of the ANN for predicting daily GR

Figure

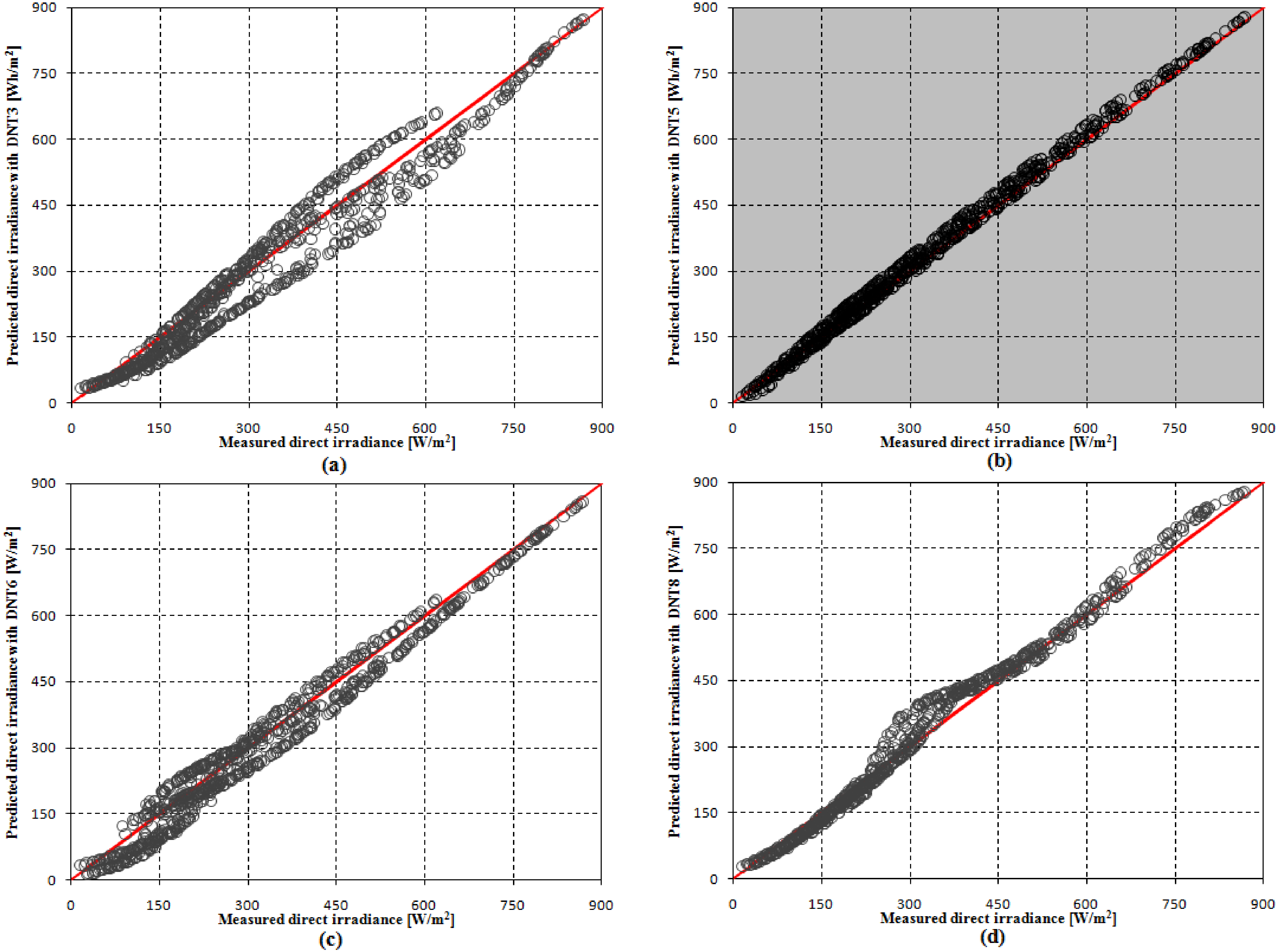

Figure 4 Scatterplots of four different configurations of the ANN for predicting hourly DNI

Figure

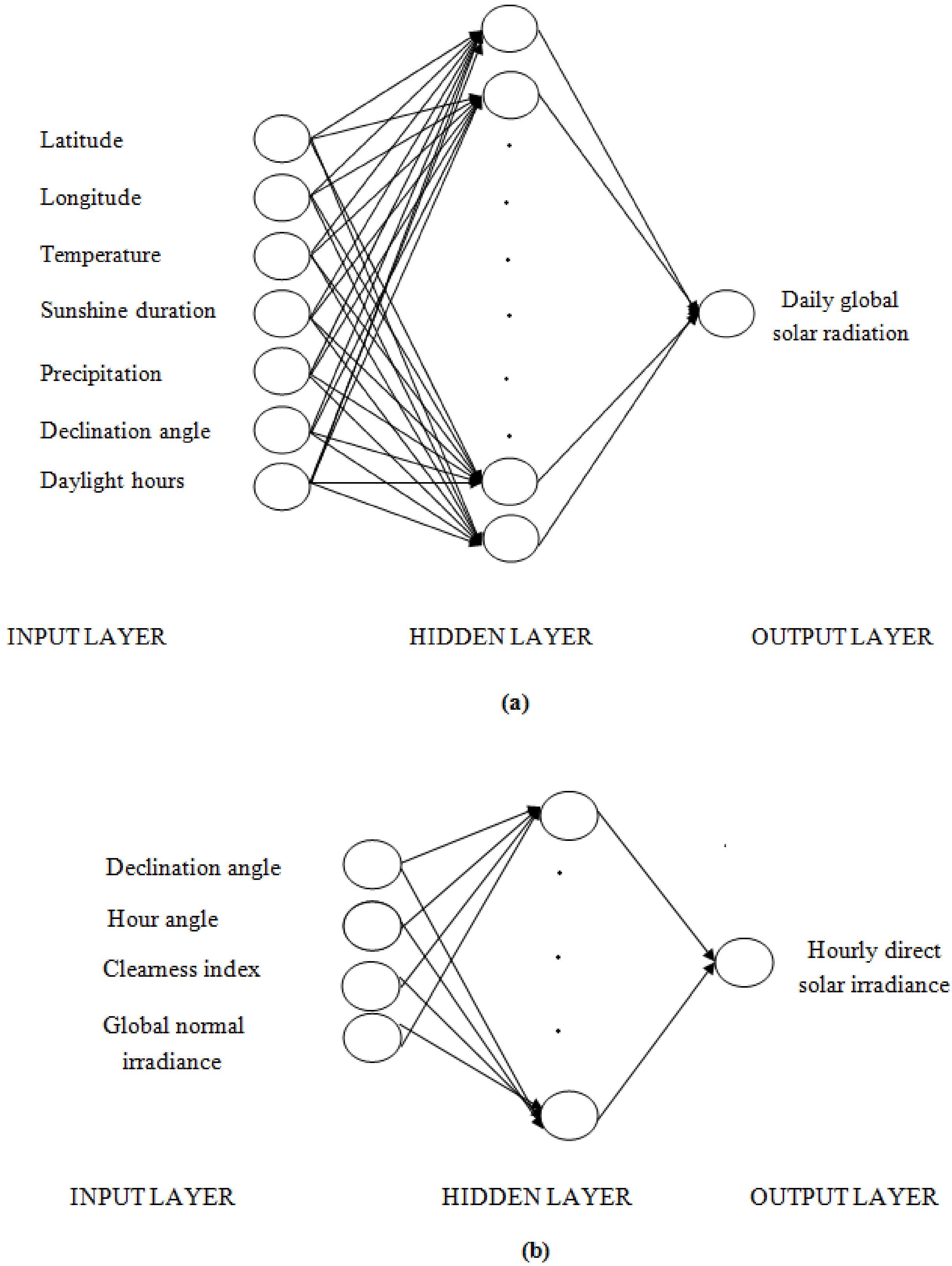

Figure 5 Structure of the proposed neural networks for: (a) daily global radiation, (b) hourly direct irradiance

Figure

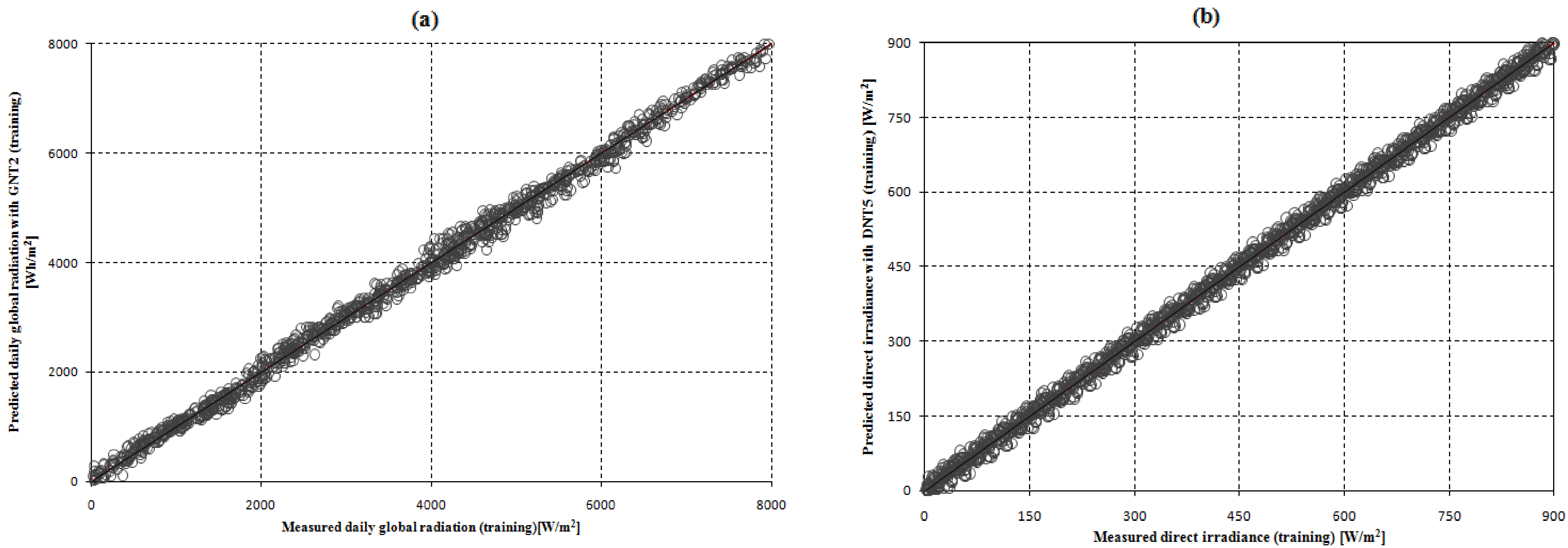

Figure 6 Regression respect to the target in the training phase: (a) GR model GNT2, (b) DNI model DNT5

Figure

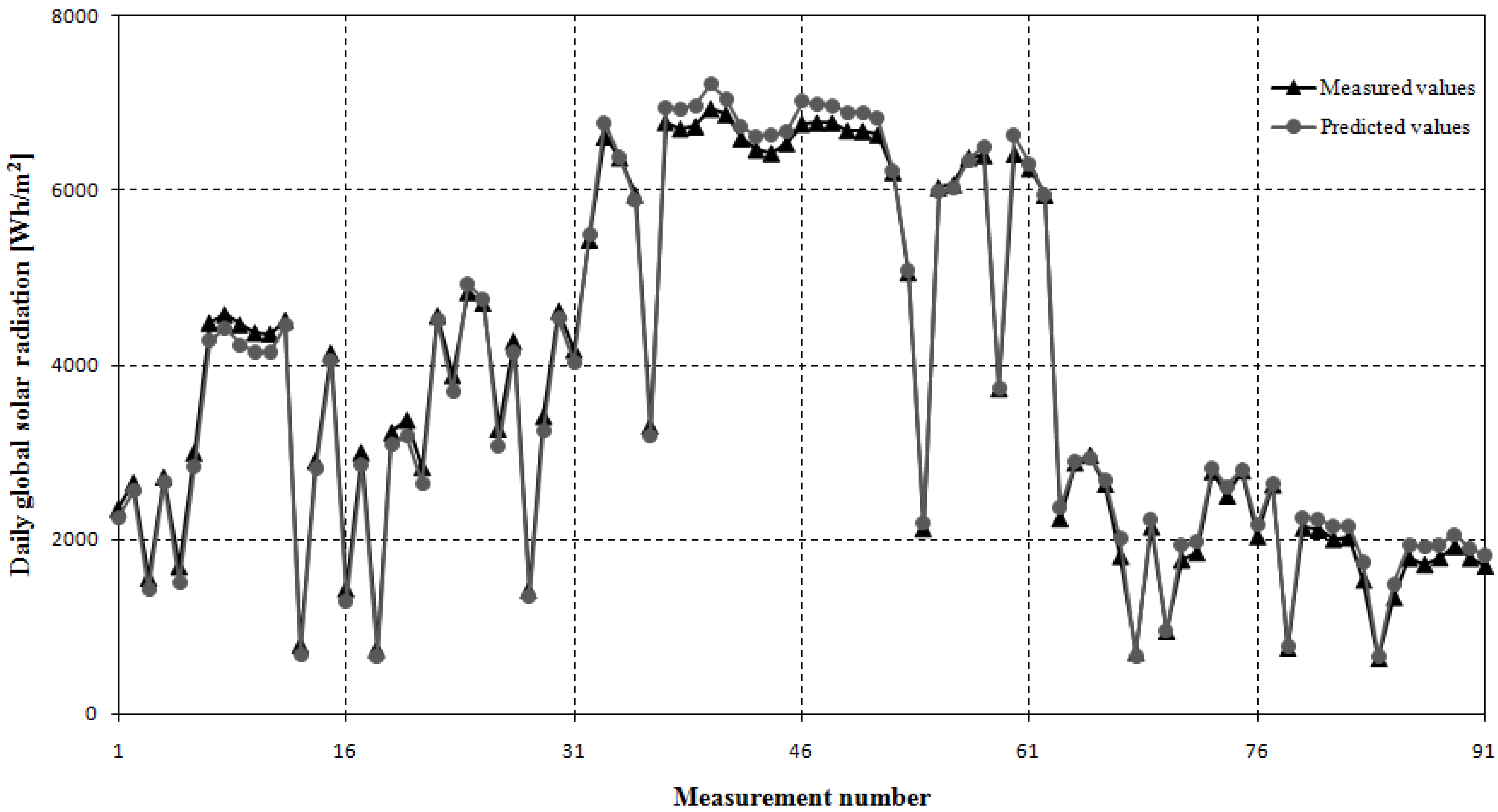

Figure 7 Comparison between measured and predicted daily GR values for University of Salerno

Figure

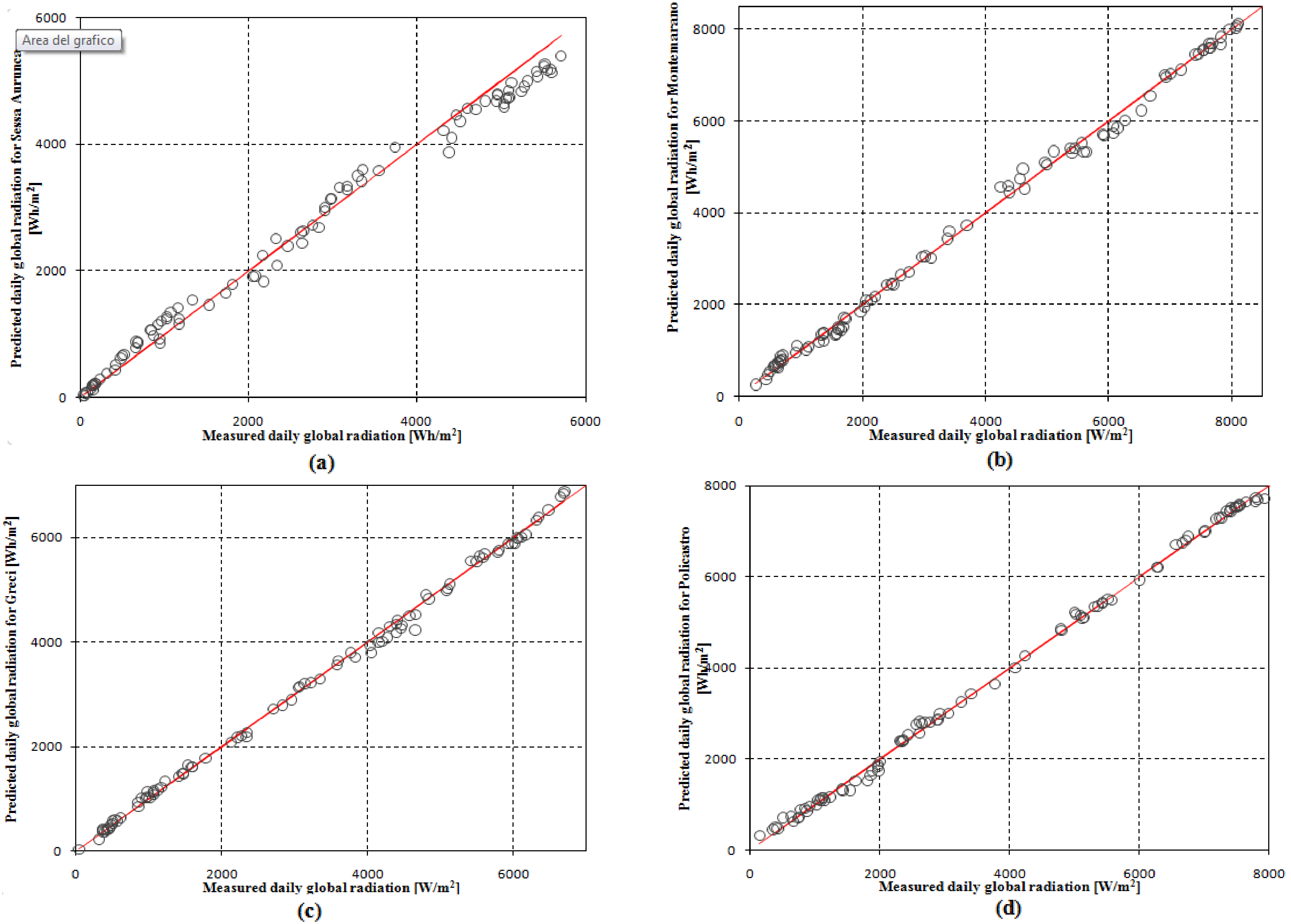

Figure 8 Comparison between measured and predicted daily GR values for different locations: (a) Sessa Aurunca, (b) Montemarano, (c) Greci, (d) Policastro Bussentino

Figure

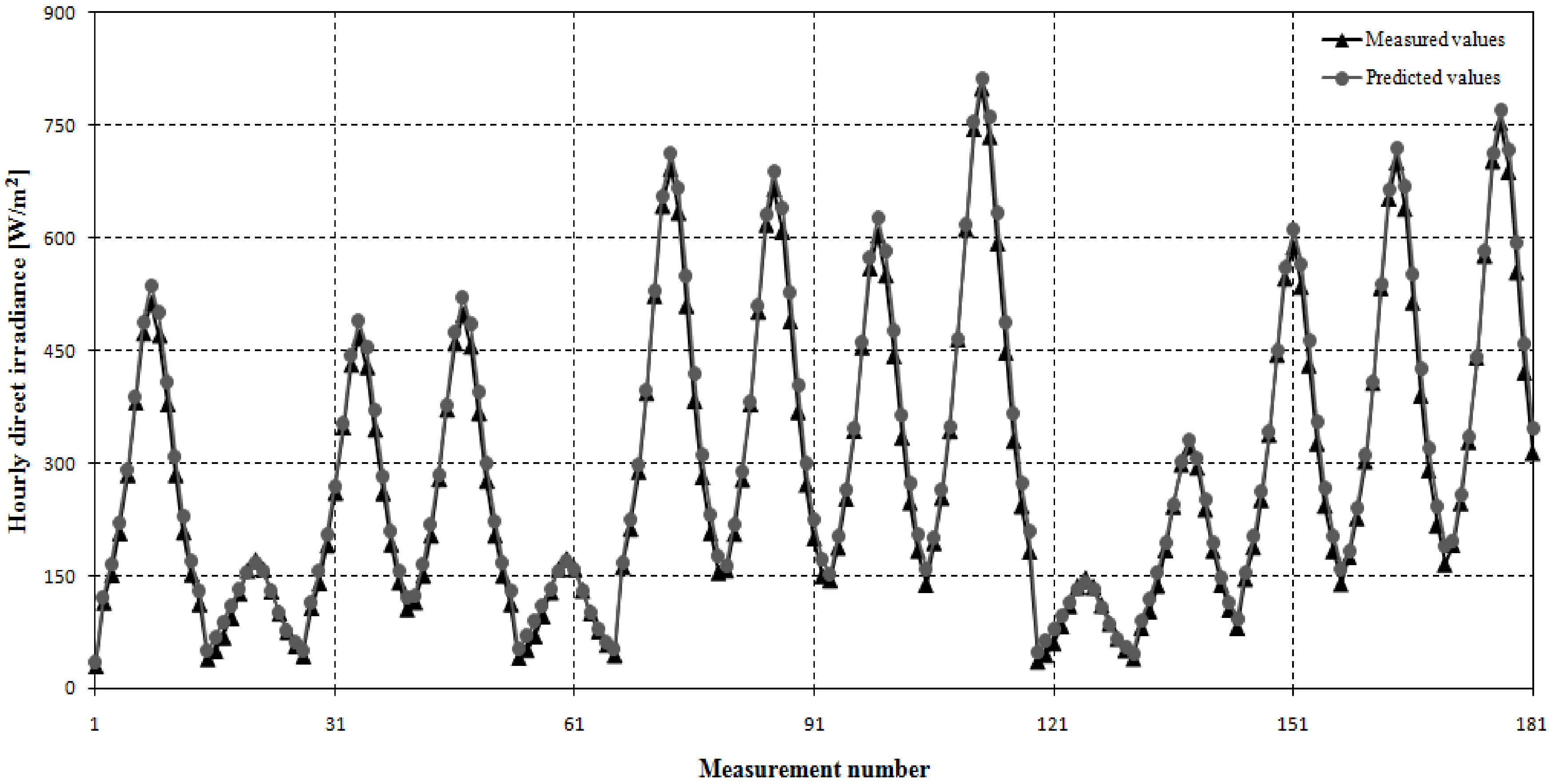

Figure 9 Comparison between measured and predicted hourly DNI values

Figure

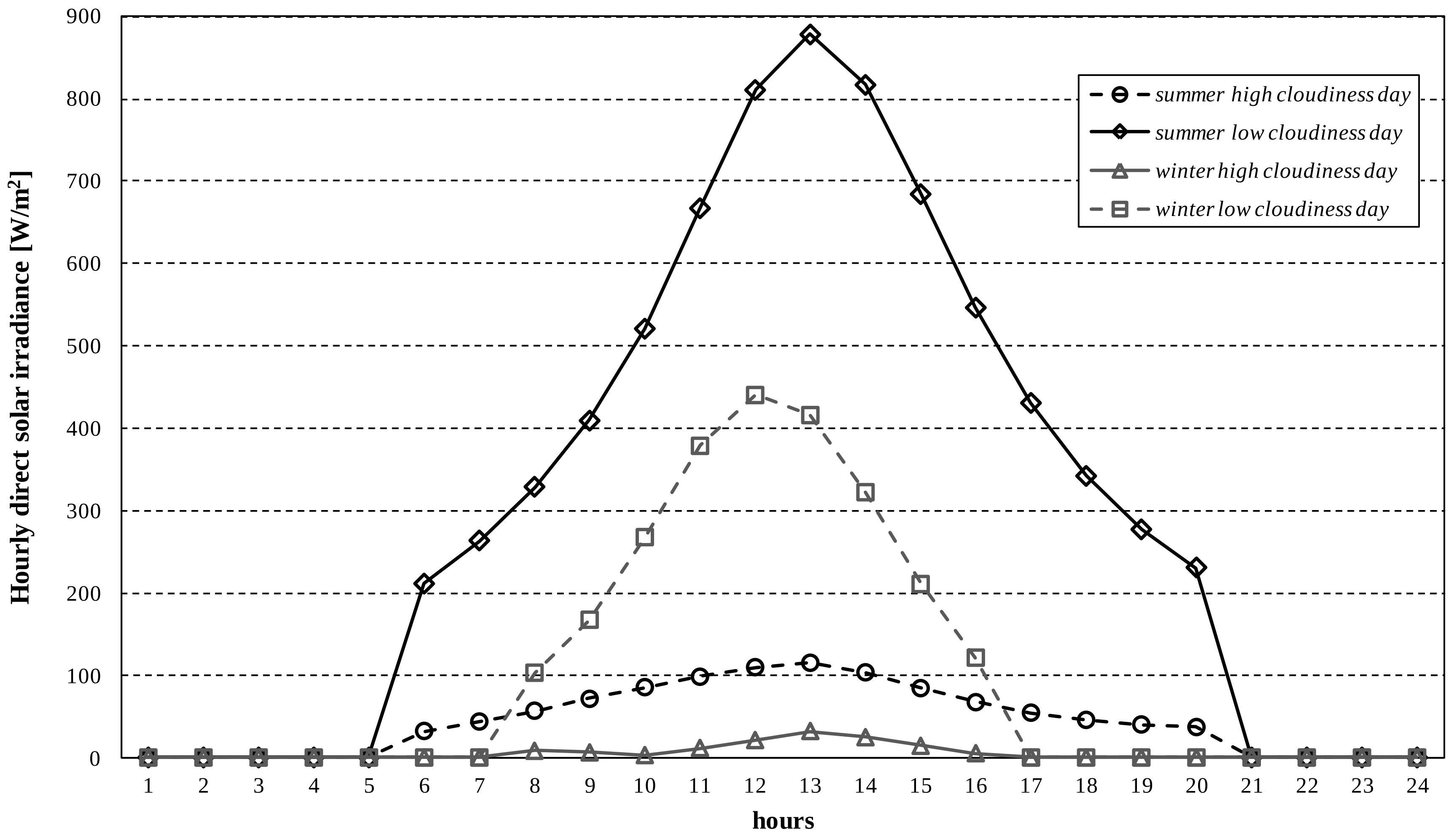

Figure 10 Hourly DNI in different climatic conditions

Figure

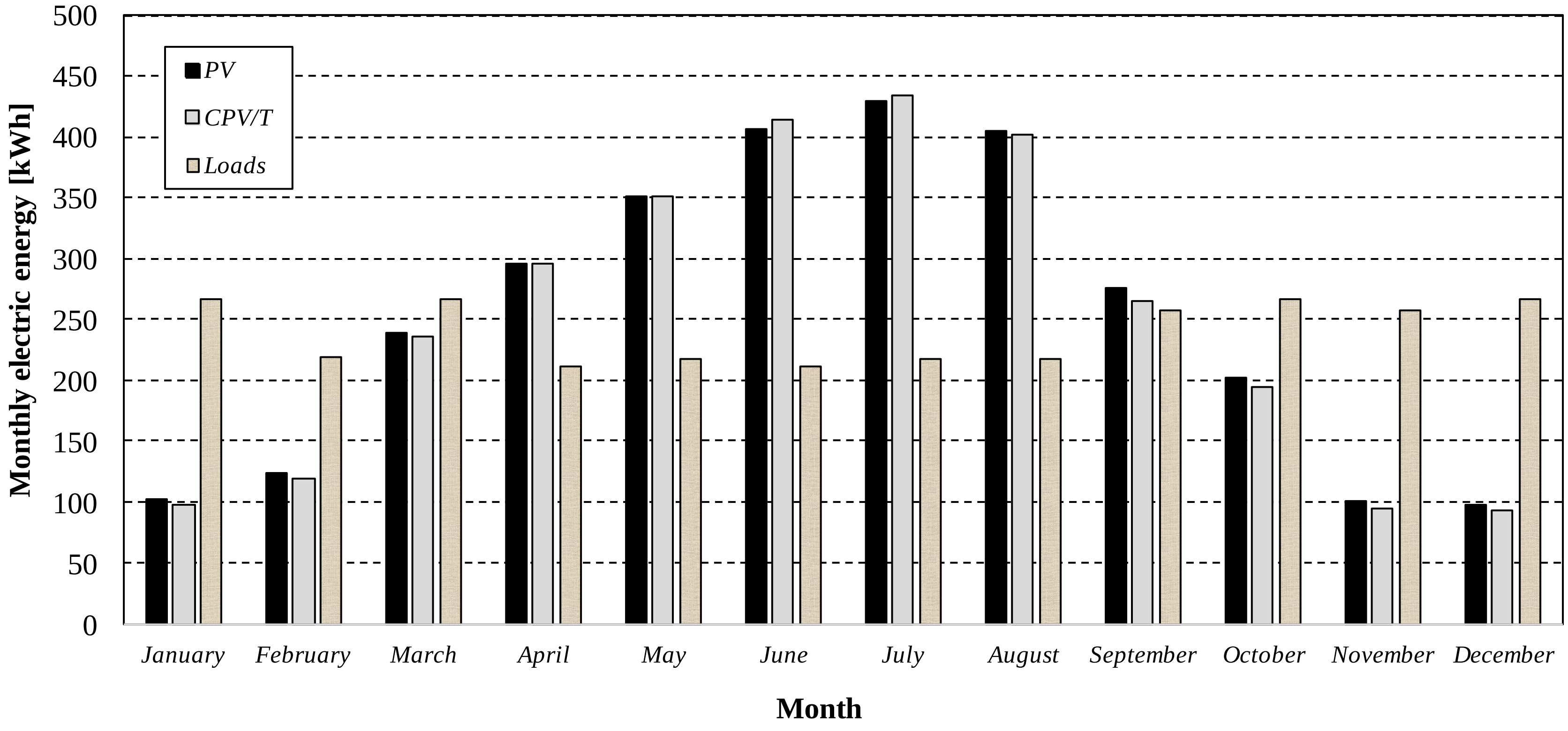

Figure 11 Electric energy demand of the residential building and monthly electric energy production of the PV and CPV/T systems

Table

Table 1 ANN characteristics summary of the literature analysis.

Model	*Networks*	*No. hidden layers*	*No. hidden neurons*	*Training algorithm*	*Variables*	*Time level*	*Parameter of interest*	*Pros*	*Cons*
Azadeh et al. 2009	MLP	1	4	BP with momentum, pruning and weight decay	AV max T, AV min T, mean RH, mean VP, P, mean WS and mean SD	monthly	GR	1. Model tested for six different cities 2. Comparisons with the Angstrom model	1. Only monthly analysis conducted 2. Less performance for some cities
Wang et al. 2011	MLP	2	18 - 13	LM	6:00 am to 8:00 pm solar irradiance	hourly	GR	1. Data pretretament 2. Error analysis in order to choose the best ANN configuration	1. No application or comparisons 2. Lack of testing for different locations
Khatib et al. 2012	MLP	1	-	BP	L_t, L_g, day number and sunshine ratio	daily	GR	1. Low number of input required (4) 2. Data from different location used for training and test	1. Indirect estimation of GR using the clearness index 2. It seems that the prediction is less accurate for very high values (high MSE)
Behrang et al. 2010	MLP and RBF	2, 1	3 - 3, 18	LM	Mean T, RH, SD, evaporation and WS	daily	GR	1. The effect of each meteorological variable is considered using six different input combinations 2. Comparison between different prediction models	1. Model tested only for Dezful (Iran)
Zervas et al. 2008	RBF	1	16	fuzzy proposed by Sarimveis [22]	Weather conditions and the duration of daylight	daily	GR	1. Less input information required 2. Investigation of the correlation between input and output using a Gaussian function	1. Subjective definition of weather condition 2. Model tested only for (37°58'26"N, 23°47'16"E)
Benghanem et al 2010	MLP and RBF	1,1	from 2 to 5, from 4 to 7	least squares approach	Day of the year, T, SD and RH	daily	GR	1. Lower nRMSE 2. Development of an application for estimating the sizing of a stand-alone PV system	1. Model tested only for Al-Madinah (Saudi Arabia) 2. The choice of the topological characteristics is not proved
Yacef et al. 2012	MLP and BNN	1,1	20, 2	LM	T, RH, SD and extraterrestrial irradiation	daily	GR	1. Development of a different ANN (BNN) 2. Comparisons beetween BNN, MLP and empirical models	1. Lesser model agreement 2. Model tested only for Al-Madinah (Saudi Arabia)
Amrouche et al.2014	two MLP	2	20 - 12	BP	temperature and global horizzontal irradiance	daily	GR	1. The models are tested for two locations 2. Trainig phase conducted using	1. No application is provided

								data from different locations (4)	
Bilgili et al. 2011	MLP	1	10	LM	SD, T, WS and date of the year	daily	GR	1. Development of different prediction model: MLP, multi linear regression and multi non-linear regression 2. Evaluation of the input importance using "Stepwise" method	1. Less model agreement 2. Model tested only for Adana (Turkey)
Mellit et al. 2013	MLP	1	15	LM	Hourly T, RH, SD and irradiance	hourly	DNI	1. Models for the prediction of global, direct and diffuse radiation 2. Comparison between the feed-forward model and an adaptive model	1. Less value of R^2 2. Model tested only for Jeddah (Saudi Arabia)
Kaushika et al. 2014	feed-forward	1	14	-	L_t, L_g, altitude, month, local mean time, monthly mean hourly rainfall, monthly mean hourly HR, monthly mean SD	monthly	DNI	1. Very accurate DNI estimation 2. For the model development they have been employed data from different stations	1. Indirect estimation of DNI using the clearness index 2. High number of input parameter

Table

Table 2 Correlation analysis for GR model input

Variables	***Correlation to GR***
Latitude (Lt)	0.241
Longitude (Lg)	0.241
Mean Temperature (T)	0.667
Sunshine Duration (SD)	0.974
Precipitation (P)	-0.767
Declination angle (δ)	0.788
Daylight hours (H)	0.786
Humidity (Hu)	-0.611
Wind speed (WS)	-0.524

Table

Table 3 Number of input and nRMSE for the GR model

	No. Input	***Input***	***nRMSE***
1	5	Lt, Lg, SD, T, P	0.090
2	5	Lt, Lg, SD, T, δ	0.095
3	5	Lt, Lg, SD, T, H	0.106
4	5	Lt, Lg, SD, T, HR	0.143
5	5	Lt, Lg, SD, T, W	0.154
6	6	Lt, Lg, SD, T, P, δ	0.043
7	6	Lt, Lg, SD, T, P, H	0.050
8	6	Lt, Lg, SD, T, P, HR	0.063
9	6	Lt, Lg, SD, T, P, W	0.069
10	6	Lt, Lg, SD, T, δ, H	0.046
11	6	Lt, Lg, SD, T, δ, HR	0.066
12	6	Lt, Lg, SD, T, δ, W	0.092
13	6	Lt, Lg, SD, T, H, HR	0.087
14	6	Lt, Lg, SD, T, H, W	0.101
15	6	Lt, Lg, SD, T, HR, W	0.134
16	7	Lt, Lg, SD, T, P, δ, H	0.018
17	7	Lt, Lg, SD, T, P, δ, HR	0.055
18	7	Lt, Lg, SD, T, P, δ, W	0.089
19	7	Lt, Lg, SD, T, δ, H, HR	0.072
20	7	Lt, Lg, SD, T, δ, H, W	0.092
21	7	Lt, Lg, SD, T, H, HR, W	0.105

Table

Table 4 Different topology configurations of the ANN model for daily GR

ANN models for daily global radiation			
Network topology	*Transfer functions*	*Number of hidden layers*	*Number of hidden neurons*
GNT 1	sigmoid - linear	1	8
GNT 2	sigmoid - linear	1	10
GNT 3	sigmoid - linear	1	12
GNT 4	tanh - tanh	1	8
GNT 5	tanh - tanh	1	10
GNT 6	tanh - tanh	1	12
GNT 7	tanh - tanh - linear	2	6 - 4
GNT 8	tanh - tanh - linear	2	5 - 3
GNT 9	tanh - tanh - linear	2	7 - 5

Table

Table 5 Correlation analysis for DNI model input

Variables	***Correlation to DNI***
Hour angle (HRA)	-0.505
Glomal normal irradiance (Gni)	0.985
Clearness index (Kt)	0.929
Declination angle (δ)	-0.657

Table

Table 6 Number of input and nRMSE for the DNI model

	No. Input	***Input***	***nRMSE***
1	3	G_{gi}. HRA. K_t	0.0458
2	3	G_{gi}. HRA. δ	0.0328
3	3	G_{gi}. K_t. δ	0.0191
4	4	G_{gi}. HRA. K_t. δ	0.00967

Table

Table 7 Different topology configurations of the ANN model for hourly DNI.

ANN models for hourly direct irradiance			
Network topology	*Transfer functions*	*Number of hidden layers*	*Number of hidden neurons*
DNT 1	tanh - tanh	1	4
DNT 2	tanh - tanh	1	5
DNT 3	tanh - tanh	1	6
DNT 4	sigmoid - linear	1	4
DNT 5	sigmoid - linear	1	5
DNT 6	sigmoid - linear	1	6
DNT 7	tanh - tanh - linear	2	4 - 2
DNT 8	tanh - tanh - linear	2	3 - 2
DNT 9	tanh - tanh - linear	2	5 - 3

Table

Table 8 Calculated statistical parameters for different network topology in ANN model for GR

Evaluation of ANN models for global radiation				
Configuration	RMSE [Wh/m^2]	MAPE [%]	MAE [Wh/m^2]	R^2
GNT 1	568.0	24.8	501.7	0.9898
GNT 2	153.5	4.46	125.7	0.9923
GNT 3	473.2	21.6	371.2	0.9802
GNT 4	584.8	21.1	471.8	0.9928
GNT 5	341.8	7.59	278.2	0.9970
GNT 6	1033	20.1	847.0	0.9841
GNT 7	348.8	7.49	270.7	0.9926
GNT 8	592.3	12.1	469.3	0.9913
GNT 9	414.1	10.9	336.5	0.9882

Table

Table 9 Calculated statistical parameters for different network topology in ANN model for DNI

Evaluation of ANN models for direct irradiance				
Configuration	RMSE [Wh/m^2]	MAPE [%]	MAE [Wh/m^2]	R^2
DNT 1	18.4	8.08	15.6	0.9938
DNT 2	18.9	7.30	16.6	0.9949
DNT 3	45.1	14.1	36.5	0.9563
DNT 4	20.3	8.27	16.8	0.9955
DNT 5	17.1	5.38	13.4	0.9956
DNT 6	34.8	15.0	30.5	0.9745
DNT 7	30.7	10.5	26.2	0.9892
DNT 8	26.0	8.06	20.1	0.9883
DNT 9	49.2	17.3	42.5	0.9574

Table

Table 10 Monthly direct fraction of global radiation.

Month	*Monthly Direct Radiation [kWh/m²]*	*Monthly Global Radiation [kWh/m²]*	*Monthly Diffuse Radiation [kWh/m²]*	*Direct fraction [%]*
January	35.87	45.22	8.67	79.3%
February	43.73	54.36	9.81	80.5%
March	87.72	104.7	15.5	83.7%
April	110.6	129.9	17.3	85.2%
May	134.2	154.4	17.9	86.9%
June	161.4	178.6	14.6	90.3%
July	169.6	188.2	15.8	90.1%
August	157.4	177.5	17.4	88.7%
September	102.9	121.0	16.2	85.1%
October	74.13	88.85	13.9	83.4%
November	35.39	44.57	8.51	79.4%
December	34.03	43.06	8.39	79.0%

Table

Table 11 User energy loads and different systems energy production.

	Energy Loads			PV System Energy	CPV/T System Energy	
Month	***Electric [kWh$_e$]***	***Thermal SHW [kWh$_{th}$]***	***Cooling [kWh$_{cool}$]***	***Electric [kWh$_{el}$]***	***Electric [kWh$_{el}$]***	***Thermal [kWh$_{th}$]***
January	267.2	324.9	0.00	103.0	97.71	331.1
February	219.4	296.3	0.00	123.8	119.1	406.2
March	267.2	324.9	0.00	238.6	235.2	814.7
April	211.6	306.1	0.00	295.8	295.5	1028
May	218.6	304.6	0.00	351.7	351.6	1247
June	211.6	283.4	512	406.9	414.6	1499
July	218.6	284.3	1089	428.7	433.7	1576
August	218.6	281.2	1089	404.2	402.5	1462
September	258.6	275.1	512	275.6	264.5	956.0
October	267.2	292.9	0.00	202.4	194.4	688.5
November	258.6	294.8	0.00	101.5	94.67	328.7
December	267.2	316.3	0.00	98.07	92.56	316.4
Total	2884	3585	3202	3030	2996	10655

Table

Table 12 Literature comparison for proposed ANN models

Literature Comparison (ANN for daily GR)						
Models	**MSE [Wh^2/m^4]**	**MAPE [%]**	**MAE [Wh/m^2]**	**R^2**	**RMSE [Wh/m^2]**	**nRMSE [%]**
Proposed	25696	4.57%	131.2	0.9918	160.3	3.54%
Azadeh et al. [22]	-	3.00%	-	0.980	-	2.60%
Wang et al. [23]	-		-	0.991 ; 0.964	-	3.31% ; 4.50%
Khatib et al. [24]	135719	5.20%	-	-	342.0	7.96%
Behrang et al. [25]	-	5.21% ; 5.56%	-	0.9957 ; 0.9952	-	-
Zervas et al. [26]	-	-	-	0.985	-	-
Benghanem et al. [27]	-	-	-	0.976	-	1.31%
Yacev et al. [28]	-	-	-	0.9299	-	8.42%
Bilgili et al. [30]	-	9.23%	278.0	0.9508	-	-

ANN for hourly DNI			
Model	**MAPE [%]**	**RMSE [W/m^2]**	**R^2**
Proposed	5.57	17.7	0.994
Mellit et al. [33]	-	-	0.967
Kaushika et al. [34]	-	14.5	-